

Response to Reviewers 4/1/2024

Submission: “Isotopomer labeling and oxygen dependence of hybrid nitrous oxide production” [Manuscript ID egosphere-2023-2642]

We thank the Editor and Reviewers for their time spent reviewing this manuscript and helping to improve it. We hope that the depth of this response to reviewers file reflects the thorough consideration the reviewers’ suggestions. We provide a table of contents to aid in navigation.

Table of Contents

<i>Reviewer 1</i>	<i>1</i>
<i>Reviewer 2</i>	<i>16</i>
<i>Reviewer 3</i>	<i>26</i>
<i>Community Comment, Julie Granger</i>	<i>33</i>
<i>References</i>	<i>52</i>

This Response to Reviewers file provides complete documentation of the changes made in response to each individual Reviewer comment. The document is designed so that these changes can be immediately read and understood, independent of the other comments and responses. While this comprehensive comment-by-comment explanation requires some duplication of material throughout the document, our intention is to help evaluate easily and effectively how each individual comment has been addressed.

Reviewer comments are shown in plain text. Author responses are shown in **bold**. Quotations from the revised manuscript are shown in *italics*.

Reviewer 1

General comments

This paper reports potential rates of N₂O production by several important pathways in the oxygen deficient zone in the Eastern Tropical North Pacific. The studied oceanic region is one of the major N₂O sources to the atmosphere, and therefore this work is crucial in understanding the origin of excess N₂O and predicting the future emission of this global-warming and ozone-depleting gas under changing oceanic environment.

The strong point of this paper is that the N₂O production rate and its dependence on dissolved oxygen concentration are determined for each of the possible N₂O formation processes using ¹⁵N-labeled substrates and isotopocule measurements. The authors found the significant contribution from hybrid N₂O production during ammonia oxidation in the near-surface and deep N₂O concentration maxima. They also found that the hybrid N₂O formation is enhanced in low-oxygen water and that N₂O can be produced by denitrification from nitrate even with oxygen concentrations higher than those considered to inhibit denitrification. I believe these findings will help us develop a clear picture of N₂O cycling in and around the ODZ.

Thank you for this positive and thorough assessment of our work.

However, I think this work has a couple of drawbacks. First, the authors use conventional second-order kinetics to analyze N₂O production processes in order to calculate the rate of each pathway from the N₂O isotopocule ratios obtained by the ¹⁵N-incubation experiments. Considering that the amount of tracers added is sufficiently higher than those in initial seawater, I don't think it is always appropriate to assume that the rate is proportional to the concentration of substrates. I would like to see some justification or evidence on this assumption.

If we understand the reviewer's comment correctly, the concern is that the rates of N₂O production could have plateaued and not continued to increase (or decrease) with increasing (decreasing) substrate concentrations. In other words, the question is, what happens when you scale the N₂O production rate to the substrate concentration instead of assuming that the rate has hit its maximum value?

There are two important things to clarify:

- 1) The model solves for the 2nd-order rate constant that best fits the data, given a certain concentration of substrate. These 2nd order rate constants are not necessarily applicable to ambient substrate concentrations; thus, we report the rates, not the rate constants.**
- 2) The substrate concentrations in eqns. (13) and (14) are the total concentration of substrate including the tracer and carrier additions, not just the ambient concentrations of each substrate. Because these substrate concentrations do not vary much in the incubations, eqns. (13) and (14) effectively amount to the same thing as assuming N₂O production has plateaued and hit a maximum rate. Nonetheless there are some cases where the substrate concentrations change over the course of an incubation, and we assess below how this would influence our results.**

The experiment with the highest rates of ammonia oxidation was at station PS3, feature "interface2" (63m, Table S1). Here, the rates of ammonia oxidation were 4.68 nM/day (Table S2). In the ¹⁵N-NH₄⁺ experiment, the starting ammonium concentration was 0.52 μM, and the starting nitrite concentration was 1.61 μM. This includes the ¹⁵N-NH₄⁺ tracer addition and ¹⁴N-NO₂⁻ carrier addition. Then, the modeled hybrid N₂O production rate declines by 1% over the course of the experiment:

$$\frac{(0.52 - 0.00468)(1.61 + 0.00468)}{(0.52)(1.61)} \cdot 100 = 99\%$$

Likewise, the modeled N₂O production from solely ammonium declines by 2%:

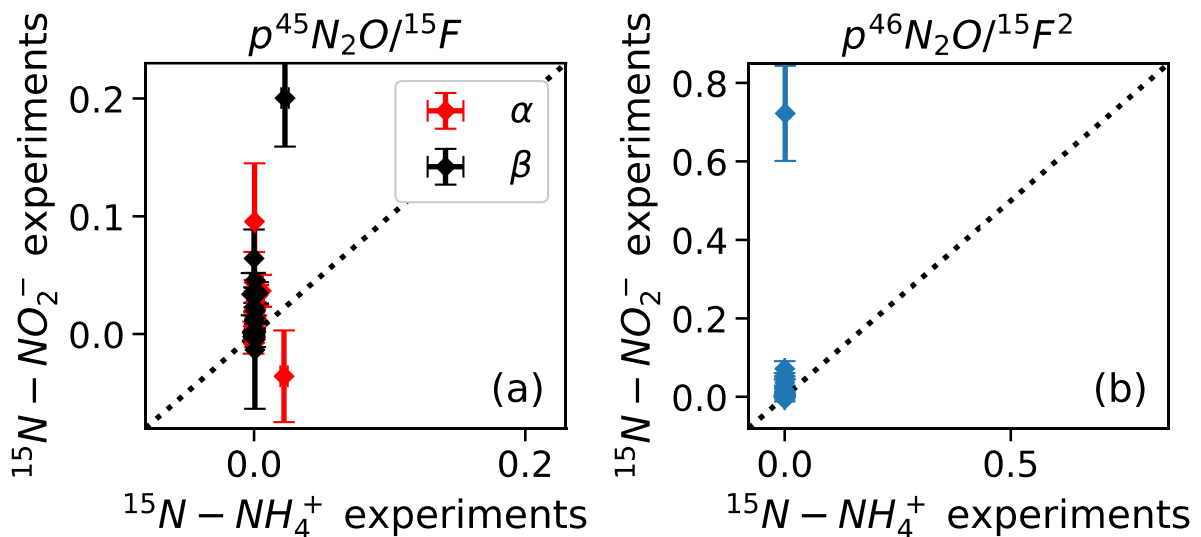
$$\frac{(0.52 - 0.00468)(0.52 - 0.00468)}{0.52^2} \cdot 100 = 98\%$$

And the modeled rate of N₂O production from NO₂⁻ increases by 0.5%:

$$\frac{(1.61 + 0.00468)(1.61 + 0.00468)}{1.61^2} \cdot 100 = 99\%$$

Even in the experiment with the highest nitrite oxidation rate, from the secondary nitrite maximum (182 m) at station PS3, the modeled rate of N₂O production from NO₂⁻ only declines by 12% over the course of the experiment, and the modeled rate of N₂O production from NO₃⁻ only increases by 4% over the course of the experiment.

What if we compare the ¹⁵N-labeled ammonium treatment to the ¹⁵N-labeled nitrite treatment at the same experimental depth, since the tracer additions were unequal (5.00 μM ¹⁵N-NO₂⁻ vs. 0.501 μM ¹⁵N-NH₄⁺)? The ⁴⁵N₂O and ⁴⁶N₂O production rates in the ¹⁵N-labeled nitrite treatment were far higher than those in the ¹⁵N-labeled ammonium treatment, even when normalized by atom fraction. This is visualized below. In fact, the rates of production of ⁴⁵N₂O and ⁴⁶N₂O in the ¹⁵N-labeled ammonium treatments were so small, comparatively, that they are visually indistinguishable from zero when plotted on the same scale as the rates of production of ⁴⁵N₂O and ⁴⁶N₂O in the ¹⁵N-labeled nitrite treatments.



Production of ⁴⁵N₂O, divided by atom fraction, in the ¹⁵N-NO₂⁻ treatment vs. ¹⁵N-NH₄⁺ treatment at the same experimental depths. Red diamonds indicate $p^{45}\text{N}_2\text{O}^\alpha/^{15}\text{F}$ and black diamonds indicate $p^{45}\text{N}_2\text{O}^\beta/^{15}\text{F}$. b) Production of ⁴⁶N₂O, divided by atom fraction squared, in the ¹⁵N-NO₂⁻ treatment vs. ¹⁵N-NH₄⁺ treatment at the same experimental depths. In both plots, the dashed line is the 1:1 line.

Since the tracer concentration was much higher in the ¹⁵N-labeled nitrite treatment (5.00 μM) than in the ¹⁵N-labeled ammonium treatment (0.501 μM), this imbalance of ⁴⁵N₂O production supports the idea that there is some dependence of N₂O production rate on substrate concentration. The 2nd order kinetics in our model allow us to capture that dependence.

Second, the contribution of suspended particulate matter to N₂O formation is not adequately taken into account in the interpretation of the results. Although the authors discuss the algal N₂O

production as an alternate source of N₂O, it seems that they do not pay more attention to other particulate matter. Why don't they consider potential N₂O production/consumption at anoxic microsites inside the particles? Although I don't know any reports on experimental evidence of such N₂O production, at least one paper suggested that active microbial CH₄ oxidation occurs within the oxic/anoxic boundary of sinking particles (Sasakawa, M. et al., 2008. JGR: Oceans, 113(C3). <https://doi.org/10.1029/2007jc004217>).

We agree with the reviewer that particle-associated denitrification is a potential alternative N₂O source, especially at the highly productive coastal station. We have added particle associated N₂O production and consumption to the discussion of potential alternative sources of N₂O.

Additionally, since our samples were unfiltered, particle associated N₂O production and consumption may have occurred in some of our experiments, especially in experiments at the highly productive coastal station. We cannot rule out any of these alternative sources of N₂O in our samples, so we consider these processes as potential contributors to the bulk denitrifying flux discussed here.

In summary, I recommend the publication of this paper after addressing the issue above and specific points below.

Specific comments

L64–66. Do the authors also mean NO does not undergo exchange with outside NO? In addition, are all the references listed here appropriate to cite? I cannot find the “evidence of nitrate reduction to N₂O without exchange with an extracellular nitrite pool” in Monreal et al. (2022) and Toyoda et al. (2023).

Yes, the process that we refer to here is N₂O production from externally sourced nitrate without exchange of intermediates outside the cell, including NO. This is the most likely mechanism explaining the large contribution of nitrate to N₂O production, but as the reviewer pointed out, it has been implied but not tested experimentally. This is implicated in both of the cited papers as a major source of N₂O in the eastern tropical North Pacific and Bay of Bengal, respectively (Monreal et al., 2022; Toyoda et al., 2023). We have clarified this in the text.

Both direct rate measurements (Ji et al., 2015, 2018; Frey et al., 2020) and natural abundance isotope measurements (Kelly et al., 2021; Casciotti et al., 2018; Monreal et al., 2022; Toyoda et al., 2023) indicate that N₂O production directly from nitrate (NO₃⁻), i.e., without exchange with extracellular nitrite (NO₂⁻) or nitric oxide (NO) pools, is the primary source of N₂O in ODZs.

L108–110. Is the STOX sensor identical with “Optode” in Table S1? It is confusing because “chemiluminescent optode” appears later in section 2.3.

Apologies for the confusion here. The measurements from STOX sensor mounted on the rosette are different from the optode measurements reported in Table S1. We have removed the mention of the STOX sensor since we do not report any of its measurements.

L131–133. I appreciate the authors’ effort to avoid oxygen contamination, but isn’t there any possibility that this procedure might reduce the oxygen concentration to the level lower than in situ seawater?

This is indeed a concern, which is why only anoxic depths (where the ambient dissolved oxygen was below detection) were purged with He gas. Depths with low but non-zero ambient oxygen were not purged. The creation of a He headspace should also result in a small reduction in the dissolved oxygen in the sample after equilibration. In this case, however, the He headspace was so small (2 mL) that it did not outweigh or even compensate for the oxygen contamination introduced during sampling. This is shown in Figure S1.

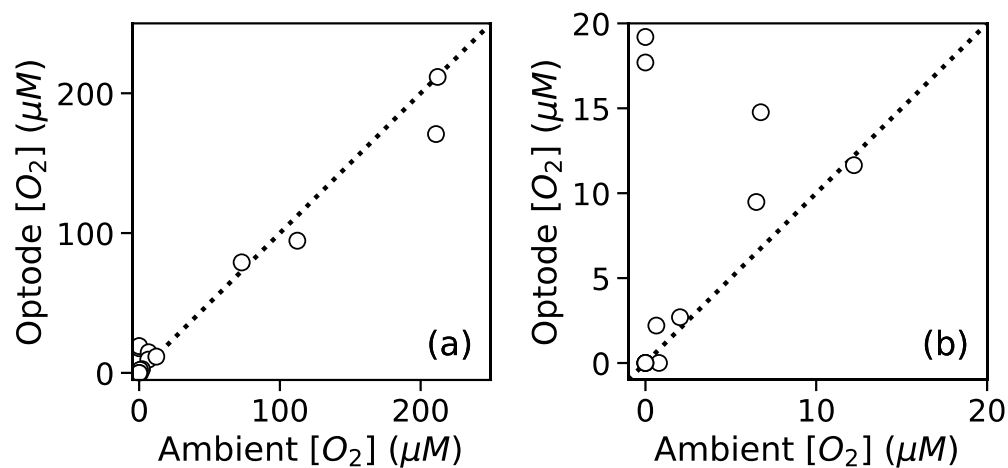


Figure S1. $[\text{O}_2]$ measured by chemiluminescent optodes mounted inside sample bottles vs. ambient $[\text{O}_2]$ measured by a Seabird sensor for the bottles from which samples were taken. Data (circles) are plotted along the full range of $[\text{O}_2]$ (a) and zoomed in to 0-20 μM $[\text{O}_2]$ (b). The dashed line in each plot is the 1:1 line. High values of optode $[\text{O}_2]$ at 0 ambient $[\text{O}_2]$ correspond to the two experiments at anoxic depths at station PS2 that were not purged before tracer addition.

L161–162. How were the fiber optic cables pulled out of the bottle without air contamination?

We apologize for the confusion. The FireSting fiber optic cables never enter the bottles, themselves. Instead, the fiber optic cables measure the signal from the oxygen sensor spot placed inside the bottles through the glass wall of the bottle. This has been clarified in the text.

At each timepoint, $[\text{O}_2]$ was measured in each sensor bottle for at least 10 minutes using fiber optic cables paired to the oxygen optode spot mounted inside the bottle (PyroScience).

L165. Could the fiber optic cables, not the sensors, be really calibrated?

The fiber optic cables were indeed calibrated with a two-point calibration, using an oxygen sensor spot mounted inside a bottle containing 30 g/L sodium sulfite solution (0% saturation) and a sensor spot mounted inside a bottle containing air-equilibrated seawater

(100% saturation). The same two calibration bottles were used for all four of the fiber optic cables, effectively correcting them to the same scale. Differences in detection limit between sensor spots were accounted for by first performing this two-point calibration procedure to correct for differences between fiber optic cables, then measuring the minimum oxygen concentration measured by each sensor spot in helium-purged seawater (purged at 100 mL/min for 90 minutes, equal to 56 volume exchanges). We have added this explanatory text.

The fiber optic cables were calibrated with a 2–point measurement of: 1) a sodium sulfite solution (30 g/L in DI, or 0.24 M) and 2) surface seawater saturated with air at 12°C (270 μM [O₂], based on a salinity = 35 psu and temperature = 12°C) (Garcia and Gordon, 1992). The two calibration bottles, each containing its own optode spot, were used to calibrate all four of the fiber optic cables, effectively correcting them to the same scale. Differences in detection limit between sensor spots were accounted for by first performing this two–point calibration procedure to correct for differences between fiber optic cables, then measuring the minimum oxygen concentration measured by each sensor spot in purged seawater (purged at 100 mL/min. for 90 minutes, equal to 56 volume exchanges). Those detection limits were specific to each optode spot and varied from 146 – 880 nM [O₂].

L177. Which does this optode mean, STOX or chemiluminescent? (see above)

Again, apologies for the confusion. We refer here to the chemiluminescent optode measurements and have removed any mention of the STOX sensor from the text.

L233–238. Because the sample for N₂O measurements were poisoned with HgCl (L151), remaining sample could damage the denitrifying bacteria. How did the authors get around this problem?

Samples are diluted in the denitrifier media (2.0 mL of sample with HgCl₂ into 5.0 mL total volume with denitrifying medium), so that the effective concentration of HgCl₂ that the denitrifiers experience is lower than typical for poisoning. In addition, the denitrifier method uses a high concentration of bacteria (denitrifiers grow in 440 mL medium for 5-7 days and are concentrated 10 times prior to using them to convert NO_x to N₂O); no adverse effects from use of HgCl₂ have been observed.

In test runs, we found no statistically significant difference in the $\delta(^{15}\text{N})$ of standards (USGS32, USGS34, and USGS35) prepared with and without HgCl₂. This was true of standards prepared with 20 nmol NO₃⁻ and 10 nmol NO₃⁻.

L269. Why were not individual uncertainties for $\delta(^{15}\text{N-NO}_2^-)$ measurements estimated? Was there no need to apply the procedure for $\delta(^{15}\text{N-NO}_2^-)$ because of larger peak area obtained?

Our method of estimating individual uncertainties was developed to deal with low NH₃ oxidation rates, which generated low peak areas in $\delta(^{15}\text{N-NO}_3^-)$ samples. Since the rates of NO₃⁻ reduction were generally much higher than the rates of NH₃ oxidation (Table S2), a parallel method was not needed to estimate individual uncertainties in samples measured with the azide method, i.e. $\delta(^{15}\text{N-NO}_2^-)$ measurements. This has been clarified in the text.

Our method of estimating individual uncertainties was developed to deal with low NH₃ oxidation rates, which generated low peak areas in $\delta(^{15}\text{N}-\text{NO}_3^-)$ samples. Since the rates of NO₃⁻ reduction were generally much higher than the rates of NH₃ oxidation (Table S2), a parallel method was not needed to estimate individual uncertainties in samples measured with the azide method, i.e. $\delta(^{15}\text{N}-\text{NO}_2^-)$ measurements, so rates of NO₃⁻ reduction were with an ordinary least squares regression in eqn. (7) instead of a weighted least squares regression.

L317. In the work by Frey et al. (2023), time course of N₂O production was analyzed with Michaelis-Menten kinetics and K_m values of 0.017–0.018 mM were obtained for oxycline at stations PS2 and PS3. In the present study, NH₄⁺ was added at 0.5 mM, two orders of magnitude higher than the K_m values. This means the rate of N₂O production should reach to the maximum value, irrespective of substrate concentration.

Please see response above regarding the representation of N₂O production kinetics in our model.

L336, eq (16). Following the convention used for eq (14), 1/2 of the right-hand side of this equation should correspond to the ammonia consumption rate.

Eq. (14) contains the factor 1/2 because that converts the rate of ammonia consumption in nM-N/day to N₂O production in nM-N₂O/day. We have clarified this in the text.

J was multiplied by 1/2 to convert the rate from nM N/day to nM N₂O/day, which was then multiplied by eqns. (9–12) to obtain the rates of production of each isotopocule (note that rates are reported in pM/day).

L566–568. Describe more details about the “different conditions”. It seems the location and cruise are identical between the two studies. Were date or time different? What were the differences in other hydrographic/chemical parameters?

It is important to note that where our samples overlapped with this previous work, we observed similar results (>90% hybrid production). The depths where we observed a smaller proportion of hybrid production had not been sampled in previous work; it is possible that we sampled different microbial communities there, acclimated to different levels of ammonium, nitrite, and dissolved oxygen. This has been clarified in the text.

Previous work in the ETNP found that hybrid N₂O production always comprised > 90% of N₂O production from NH₄⁺ (Frey et al., 2023), and where our samples overlapped with this previous work, we observed similarly high proportions of hybrid production (Fig. 5). The depths where we observed a smaller proportion of hybrid production had not been sampled previously; it is possible that we sampled different microbial communities there, acclimated to different levels of NH₄⁺, NO₂⁻, and dissolved oxygen.

L590. On the basis of which data can this claim be made? Fig. S9 shows a clear deviation from the relationship expected for N₂O production from a single substrate pool, but it does not present how the relation would be if NH₄⁺ and NO₂⁻ were used in the ratio 1:1.

That's true. We don't actually present evidence of the 1:1 ratio of NH₄⁺ to NO₂⁻; instead, hybrid N₂O production is operationally defined in our model as a 1:1 combination of N derived from NH₄⁺ and NO₂⁻, which is generally consistent with previous work (Stieglmeier et al., 2014). Any combination of N derived from NO₂⁻ with a second N derived from NO₂⁻ would be included in the N₂O production from NO₂⁻ pool; likewise, any combination of N derived from NH₄⁺ with a second N derived from NH₄⁺ would be included in the N₂O production from solely NH₄⁺ pool. The question, then, is what reaction would be specific enough to have one N derived from each substrate, but not specific enough to govern ¹⁵N placement in the resulting N₂O? One such reaction could be the combination of NH₄⁺ and NO₂⁻ to form an intermediate such as hyponitrite (HONNOH or ⁻ONNO⁻ in its deprotonated form), which reacts to form N₂O via breakage of one of the N–O bonds, resulting in N₂O that contains a 1:1 ratio of NH₄⁺: NO₂⁻. With a precursor such as hyponitrite, equal formation of ⁴⁵N₂O^α and ⁴⁵N₂O^β could be achieved with non-selective N–O bond breakage. We have revised the discussion accordingly.

In our model, hybrid N₂O production is operationally defined as a 1:1 combination of N derived from NH₄⁺ and NO₂⁻, which is generally consistent with previous work (Stieglmeier et al., 2014). Any combination of N derived from NO₂⁻ with a second N derived from NO₂⁻ would be included in the modeled quantity of N₂O production from NO₂⁻; likewise, any combination of N derived from NH₄⁺ with a second N derived from NH₄⁺ would be included in the N₂O production from solely NH₄⁺. The question, then, is what reaction would be specific enough to have one N derived from each substrate, but not specific enough to govern ¹⁵N placement in the resulting N₂O? One such reaction could be the combination of NH₄⁺ and NO₂⁻ to form a symmetrical intermediate such as hyponitrite (HONNOH or ⁻ONNO⁻ in its deprotonated form), which reacts to form N₂O via breakage of one of the N–O bonds, resulting in N₂O that contains a 1:1 ratio of NH₄⁺:NO₂⁻. With a precursor such as hyponitrite, equal formation of ⁴⁵N₂O^α and ⁴⁵N₂O^β could be achieved with non-selective N–O bond breakage.

L614–616. I cannot understand whether the authors consider the N-O bond breakage occur randomly or at specific site regardless of ¹⁵N distribution in the intermediate containing two N-O bonds. I see that the former case corresponds to $f = 1/2$, and $\delta^{15}\text{N}^{\text{sp}}$ will become equal to ϵ (i.e., ¹⁴N-O bond at one side of the intermediate molecule is more likely to be broken than ¹⁵N-O bond at the other side). In the latter case, however, what happens if the bond cleavage resulting in N^β of N₂O does not proceed due to the slower rate for ¹⁵N than ¹⁴N? We cannot rule out the possibility that the intermediate go back to substrate in such a case, but it accompanies N-N bond breakage, which should require more energy than N-O bond breakage. Rather, it appears that all intermediates are eventually converted to N₂O. Then we don't need to consider ϵ for the N^β-O bond breakage.

Here we assume the former case: that either N-O bond could break, not at a specific site.

L623–625 and 674–677. I agree that denitrification is not likely to proceed in the aerobic water column, but how about the microsites within suspended particles which might provide anaerobic condition?

Good point — it is also possible that particle-associated denitrification is a potential driver of the $\delta(^{15}\text{N}^{\text{sp}})$ minimum observed in Popp et al. (2002) (L623-625). While we have removed the discussion of Popp et al. (2002), we added particle-associated denitrification as a potential contributor to our observed N_2O production from denitrification at higher-than-expected dissolved oxygen levels (L674-677).

Most surprising were the significant rates of N_2O production via denitrification at $[\text{O}_2] > 3 \mu\text{M}$ (Fig. 8g–h), which has previously been suggested as the threshold above which denitrification ceases (Dalsgaard et al., 2014). These observations are particularly evident in the plots of N_2O production from NO_3^- vs. incubation $[\text{O}_2]$ (Fig. 8h), where positive, significant rates of N_2O production from NO_3^- were evident in incubations containing $[\text{O}_2]$ as high as $19.2 \pm 0.8 \mu\text{M}$ (PS2 Deep ODZ Core experiment). One explanation for N_2O production via denitrification at such high levels of ambient dissolved oxygen is particle-associated denitrification (Bianchi et al., 2018; Smriga et al., 2021; Wan et al., 2023a).

L632 (caption), It would be helpful if x-axis includes the full range of f (0 to 1).

We modified the x-axis to include the full range of f :

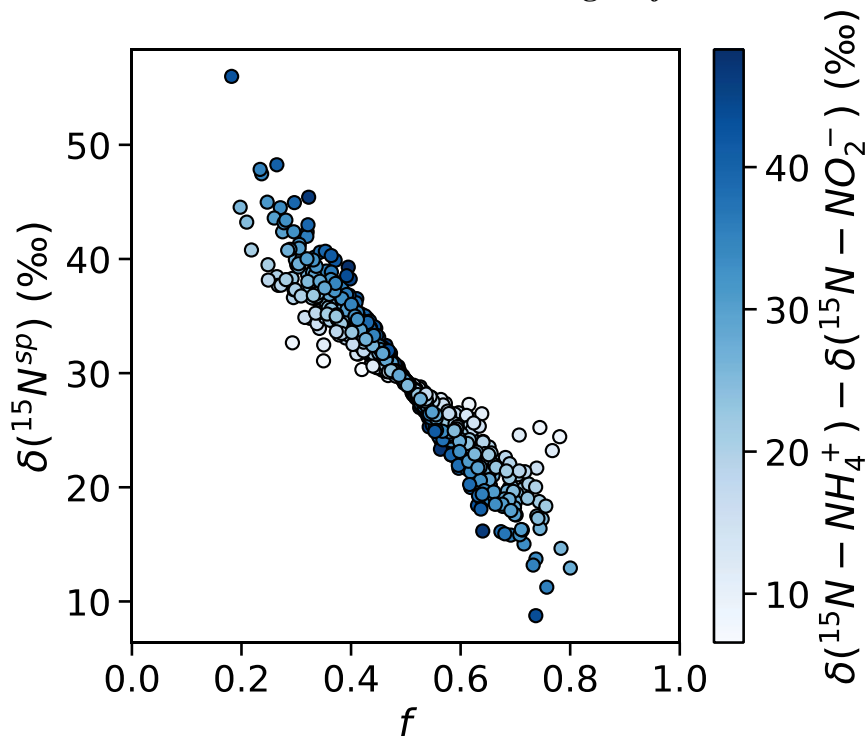


Figure 10. Simulated values of $\delta(^{15}\text{N}^{\text{sp}})$ calculated with a range of f (the proportion of N^{α} derived from NO_2^- during hybrid N_2O production) and $\delta(^{15}\text{N}-\text{NH}_4^+) - \delta(^{15}\text{N}-\text{NO}_2^-)$, assuming $\epsilon = 30.3\text{‰}$ (Santoro et al., 2011). Results are shaded by $\delta(^{15}\text{N}-\text{NH}_4^+) - \delta(^{15}\text{N}-\text{NO}_2^-)$. When f is less than or greater than $1/2$, there is the potential for $\delta(^{15}\text{N}^{\text{sp}})$ to depend on the isotopic compositions of each substrate.

L721–728. It seems that the authors assumes the first case I pointed out above. I cannot follow why the resulting site preference becomes variable.

Thank you for making this point. We rephrased the conclusions to focus on the fact that we see more or less equal production of $^{45}\text{N}_2\text{O}^\alpha$ and $^{45}\text{N}_2\text{O}^\beta$ in most of our experiments, which would imply that hybrid $\delta(^{15}\text{N}^{\text{sp}})$ does *not* vary.

Based on the equal production of $^{45}\text{N}_2\text{O}^\alpha$ and $^{45}\text{N}_2\text{O}^\beta$ in the vast majority of our experiments, we posit a two–step process for hybrid N_2O production involving an initial bond–forming step that draws nitrogen atoms from each substrate to form a symmetric intermediate, and a second bond–breaking step that breaks an N–O bond in the symmetric intermediate to form N_2O . From this, we infer that hybrid N_2O production likely has a consistent $\delta(^{15}\text{N}^{\text{sp}})$, despite drawing from two distinct substrate pools. This has important implications for the interpretation of natural abundance isotopocule measurements, since it implies that it may be possible to define a $\delta(^{15}\text{N}^{\text{sp}})$ endmember for hybrid N_2O formation. More culture experiments are needed to quantify the $\delta(^{15}\text{N}^{\text{sp}})$ of N_2O produced by ammonia–oxidizing archaea under different temperatures, oxygen levels, and ratios of $\text{NH}_4^+:\text{NO}_2^-$.

L768 (eq A10) and L769. “slope2” and “intercept2” do not appear in eq (A10). Is this equation correct?

Thank you for catching this error. Eqn. (A10) was indeed written incorrectly. We corrected eqn. (A10) to include slope_2 and intercept_2 (now called m and b).

$$\delta(^{15}\text{N}_{\text{corrected},i}) = m \left(\frac{A_{\text{sample}}}{A_{\text{measured},i}} \right) + b \quad (\text{A10})$$

Table S3. If I understand correctly, f is applicable only to hybrid N_2O production. Why values (including 0) are listed even when hybrid production rate is zero?

Thank you for catching this error. We have removed the f values in Table S3 (now table S4) and Fig. S12 (now Fig. S10) for experiments where the hybrid production rate is zero. There are some very small but significant rates that were hidden due to how the numbers were rounded. The rates in Table S4 have been converted to $\mu\text{M}/\text{day}$ to fix this issue.

Technical corrections

L24. O in N_2O should not be subscript.

Corrected.

...as well as the isotopic labeling of the central (α) and terminal (β) nitrogen atoms of the N_2O molecule.

L38. The error for the value “0.85” should be “0.03”?

Corrected.

N_2O has a global warming potential 273 times that of carbon dioxide (Smith et al., 2021), and its atmospheric mixing ratio is increasing at a rate of 0.85 ± 0.03 ppb/year (Tian et al., 2020).

L43. The “m” in “mmol/kg” must be mu.

Corrected.

ODZs have expanded over the last 60 years (Stramma et al., 2008; Breitburg et al., 2018) and will likely continue to do so as the oceans warm (Oschlies et al., 2018), although fate of the anoxic cores of ODZs ($[O_2] \leq 20 \mu\text{mol/kg}$) remains uncertain (Cabr e et al., 2015; Bianchi et al., 2018; Busecke et al., 2022).

L202, eq (3). It seems unnatural to write down $^{18}R_{VSMOW}$ numerically, but not for $^{17}R_{VSMOW}$.

Corrected.

$$^{17}R/^{17}R_{VSMOW} = (^{18}R/^{18}R_{VSMOW})^\beta [\Delta(^{17}O) + 1] \quad (3)$$

L266. Use a single character for parameters such as rate and slope.

Corrected.

$$\text{rate (nM N/day)} = \frac{m(^{15}F_{\text{product}})[P]}{^{15}F_{\text{substrate}}} \quad (7)$$

L293. nitrifier-denitrification using extracellular NO_2^- .

Corrected.

3) production from NO_2^- , i.e. denitrification or nitrifier–denitrification using extracellular NO_2^- (blue hatched horizontal arrows);

L302 (eq. 8). Subscripts “i” and “k” in the summation terms should be “n”.

Corrected.

$$N_{t+1} = N_t + \Delta t \left(\sum_{n=1}^i J_n^{\text{source}} - \sum_{n=1}^k J_n^{\text{sink}} \right) \quad (8)$$

L486 (Caption of Fig. 5). ...total N_2O production at stations PS1 (a), ...

Corrected (now Fig. 7).

Figure 7. N_2O production from solely NH_4^+ (yellow bars), hybrid N_2O production (green bars), N_2O production from NO_2^- (blue hatched bars), and N_2O production from NO_3^- (indigo bars) as proportions of total N_2O production at stations PS1 (a), PS2 (b), and PS3 (c). Data are plotted over depth profiles of dissolved $[O_2]$ (dashed lines) and $[N_2O]$ (solid lines, from Kelly et al., 2021). Note broken y–axes and different x–axis scales for $[O_2]$ and $[N_2O]$ (top) and proportions (bottom).

L506 (Caption of Fig. 6). I cannot see “values of a and b in white boxes”, but a legend (without box) showing the fitting function in each panel.

Apologies, the Copernicus system seemed to have removed any transparent objects (including these white boxes) from figures if they are saved as vector files. We removed the transparent objects to fix this issue.

L529. “0.12 nM N_2O /day” seems to correspond to “0.11” in Table S3.

0.12 was the correct number. We have changed the units of Table S3 (now Table S4) to pM N_2O /day to make the numbers easier to read.

L614. Add equation number to the first equation, or continue the eq (24) from the first line by deleting “ $\delta(^{15}\text{N}^{\text{sp}})$ ” in the left-hand side.

Corrected.

$$\begin{aligned} \delta(^{15}\text{N}^{\text{sp}}) &= \delta(^{15}\text{N}^{\alpha}) - \delta(^{15}\text{N}^{\beta}) \\ &= [f\delta(^{15}\text{N} - \text{NO}_2^-) + (1-f)\delta(^{15}\text{N} - \text{NH}_4^+)] - [(1-f)\delta(^{15}\text{N} - \text{NO}_2^-) + f\delta(^{15}\text{N} - \text{NH}_4^+) - \varepsilon] \end{aligned} \quad (24)$$

L754 (eq A2) and L755. It is confusing to use same character “m” and “b” in eq (A2) and the general equation for linear function.

Changed terms “m” and “b” to “ A_{measured} ” and “ A_{blank} ”.

$$\delta(^{15}\text{N}_{\text{measured}}) = \delta(^{15}\text{N}_{\text{sample}}) \left(\frac{A_{\text{sample}}}{A_{\text{measured}}} \right) + \delta(^{15}\text{N}_{\text{blank}}) \left(\frac{A_{\text{blank}}}{A_{\text{measured}}} \right) \quad (A2)$$

L757 and elsewhere. Parameters in equations A3–A7 and A10 should be written with a single character (and subscripts).

Corrected.

Eqn. (A2) can be expressed as a linear equation $y = mx + b$, where m is the slope of $\delta(^{15}\text{N}_{\text{measured}})$ vs. $\delta(^{15}\text{N}_{\text{sample}})$ and b is the y -intercept. Thus:

$$m = \left(\frac{A_{\text{sample}}}{A_{\text{measured}}} \right) \quad (A3)$$

$$b = \delta(^{15}\text{N}_{\text{blank}}) \left(\frac{A_{\text{blank}}}{A_{\text{measured}}} \right) \quad (A4)$$

We can obtain the mean blank peak area A_{blank} from the slope and the mean peak area of the measured reference materials (A_{measured}):

$$\left(\frac{A_{\text{blank}}}{A_{\text{measured}}} \right) = 1 - \left(\frac{A_{\text{sample}}}{A_{\text{measured}}} \right) = 1 - (m) \quad (A5)$$

$$A_{\text{blank}} = [1 - (m)](A_{\text{measured}}) \quad (A6)$$

Finally, we obtain $\delta(^{15}\text{N}_{\text{blank}})$ from:

$$\delta(^{15}\text{N}_{\text{blank}}) = b / \left(\frac{A_{\text{blank}}}{A_{\text{measured}}} \right) = \frac{b}{1 - (m)} \quad (A7)$$

L972. Fix the author lists of Prokopiou et al. (2017).

This reference has been removed.

Title page of supplement says the file contains 14 figures, but I can see only 12.

Corrected (there are now 10 supplementary figures).

Figure S1. Add “a” or “b” to each panel.

Corrected.

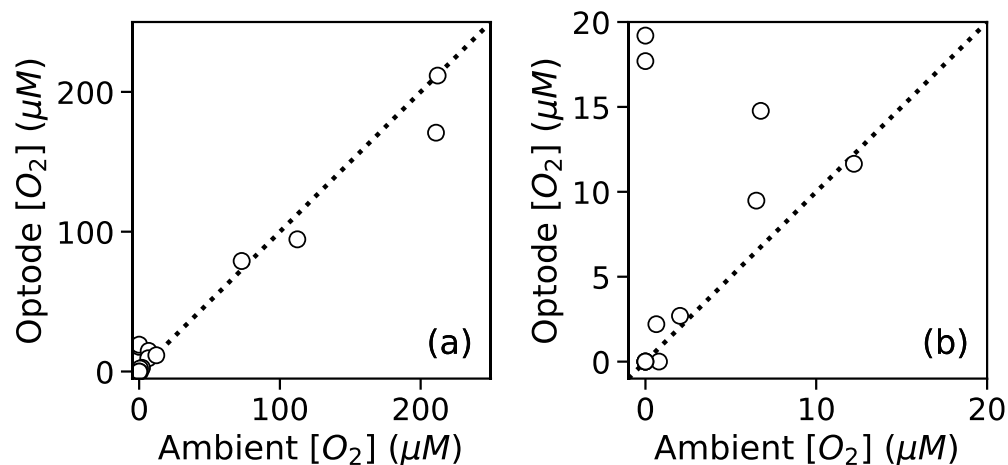


Figure S1. $[O_2]$ measured by chemiluminescent optodes mounted inside sample bottles vs. ambient $[O_2]$ measured by a Seabird sensor for the bottles from which samples were taken. Data (circles) are plotted along the full range of $[O_2]$ (a) and zoomed in to 0-20 μM $[O_2]$ (b). The dashed line in each plot is the 1:1 line. High values of optode $[O_2]$ at 0 ambient $[O_2]$ correspond to the two experiments at anoxic depths at station PS2 that were not purged before tracer addition.

Figure S2. It would be helpful if the region of ambient nitrate between 20 and 50 mM is enlarged because the delta values look significantly higher than natural values.

We added a panel (b) with values between 20 and 50 μM . They are indeed elevated.

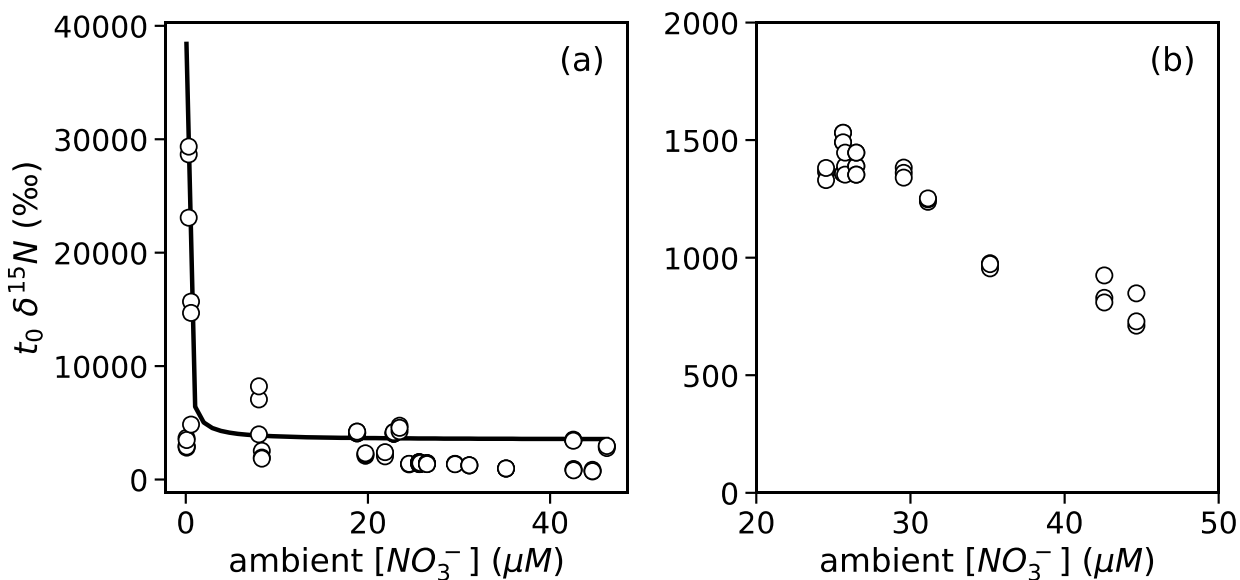


Figure S2. $\delta^{15}N-NO_x$ at t_0 vs. ambient $[NO_3^-]$ in $^{15}N-NO_2^-$ experiments across the full range of ambient $[NO_3^-]$ (a) and from 20-50 μM $[NO_3^-]$ (b).

Figure S4. Fix the explanation of panels a–d so that the figures and caption are consistent.
Corrected.

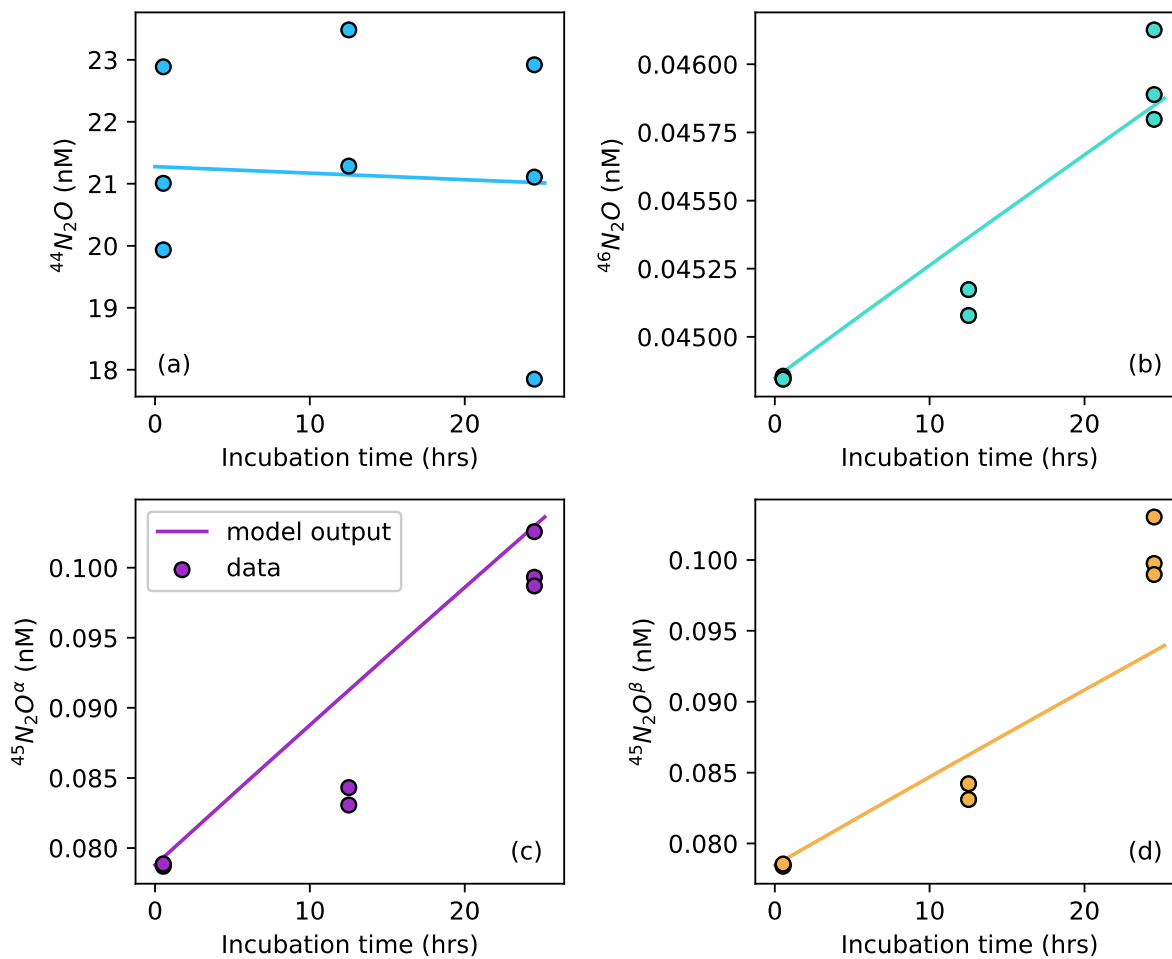


Figure S4. Example forward-running model fit through N₂O isotopocule data for the ¹⁵N-NH₄⁺ experiment in the secondary chlorophyll maximum at station PS3. Model output (solid lines) is optimized against the observed ⁴⁴N₂O (a), ⁴⁶N₂O (b), ⁴⁵N₂O^α (c), and ⁴⁵N₂O^β (d) at each timepoint in each tracer experiment.

Figure S7, caption. Fix the typo “bluen”.
Corrected.

Figure S12, caption. Panel (b) is plotted against sigma theta, not nitrite.
Corrected.

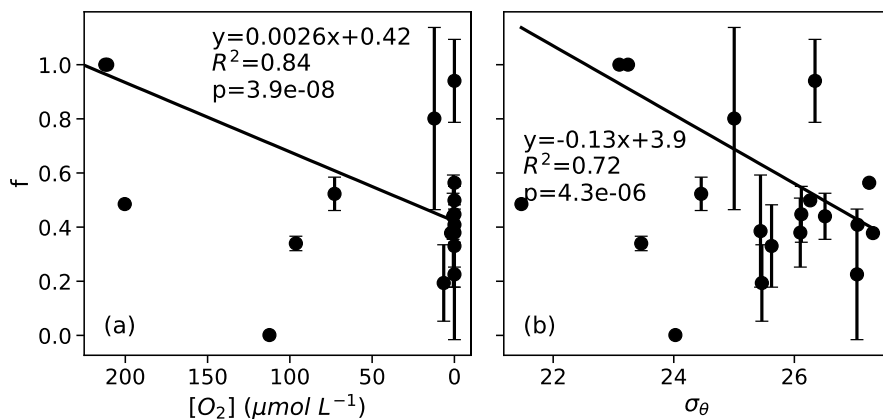


Figure S10. Weighted least squares regressions of f against ambient $[O_2]$ (a) and potential density σ_θ (b). Slope, intercept, R^2 , and p -values are displayed on each plot for the weighted least squares regression through the data. The value of f indicates the proportion of each N atom in N_2O derived from NH_4^+ and NO_2^- during hybrid N_2O production; as approaches 1, more of N^α is derived from NO_2^- . Separation of $^{45}N_2O^\alpha$ and $^{45}N_2O^\beta$ production indicate values of f less than or greater than $1/2$.

Reviewer 2

This study presents very interesting findings on N₂O hybrid production in marine environment. The complex approach applying ¹⁵N tracing methods in 3 different treatments with simultaneous measurements of d15N alfa and beta is very innovative and applied here for the first time in a real case study. Authors present the improved method of calculations of d15N alfa and beta in traced experiments, which has been integrated into the isotopomer-calculation software. These points are making this study important in further development of N₂O-isotope based research, since the presented approach may broaden our interpretation potential of N₂O isotopologue studies.

However, the manuscript needs minor revision. Due to complexity of the experimental approach and results description, some aspects are difficult to follow by the reader and some information is missing. I suggest some technical corrections for this (below).

Thank you very much for your insightful comments and suggestions! Please find our point-by-point responses below.

But more importantly, I disagree with the conclusion that hybrid N₂O formation results in incorporation of N atoms from 2 substrates into different positions of N₂O molecule (alfa and beta) - because this is not supported by your data. Most of your samples indicate the opposite - that N is located in both position independently of the substrate - which you describe very nicely in section 4.2. Below, in the specific comments, I also explain my points in more detail.

Very true. We have rephrased this part of the discussion, as well as the conclusions and abstract, to center around the fact that we *do* see equal formation of ⁴⁵N₂O^α and ⁴⁵N₂O^β in most of our experiments, which would indicate that hybrid site preference does not vary after all.

Hybrid N₂O production peaked in the same depths as NH₃ oxidation (Fig. 6c, g, k), which were also the depths at which ammonia-oxidizing archaea were most abundant (Frey et al., 2023), consistent with N₂O production associated with ammonia-oxidizing archaea. At most stations and depths, the production of ⁴⁵N₂O^α and ⁴⁵N₂O^β in both the ¹⁵N-NO₂⁻ and ¹⁵N-NH₄⁺ experiments were roughly equal. From this we conclude that during hybrid formation, N^α and N^β each retained nitrogen atoms derived from both NH₄⁺ and NO₂⁻. The equal formation of ⁴⁵N₂O^α and ⁴⁵N₂O^β led to values of f within error of 0.5 in most of our experiments (Table S4), and the mean value of f across all stations and depths was 0.5±0.2. This means that during hybrid N₂O production, half of the N^α atoms were derived from NO₂⁻, and half were derived from NH₄⁺ (likewise for N^β).

Although our data do not allow us to comment directly on the enzymatic machinery of hybrid N₂O formation, our data can be used to theorize hypothetical pathways for hybrid N₂O production. Firstly, we see much higher rates of hybrid production using ambient NO₂⁻ (Pathway 3 in Wan et al., 2023) than hybrid production using cellular NO₂⁻ (Pathway 2 in Wan et al., 2023). Again, this agrees with the results of Wan et al. (2023), who see higher rates of hybrid formation from extracellular NO₂⁻ within the range of [¹⁵N-NH₄⁺]/[NO₂⁻] covered by our

experiments. In our model, hybrid N₂O production is operationally defined as a 1:1 combination of N derived from NH₄⁺ and NO₂⁻, which is generally consistent with previous work (Stieglmeier et al., 2014). Any combination of N derived from NO₂⁻ with a second N derived from NO₂⁻ would be included in the modeled quantity of N₂O production from NO₂⁻; likewise, any combination of N derived from NH₄⁺ with a second N derived from NH₄⁺ would be included in the N₂O production from solely NH₄⁺. The question, then, is what reaction would be specific enough to have one N derived from each substrate, but not specific enough to govern ¹⁵N placement in the resulting N₂O? One such reaction could be the combination of NH₄⁺ and NO₂⁻ to form a symmetrical intermediate such as hyponitrite (HONNOH or ⁻ONNO⁻ in its deprotonated form), which reacts to form N₂O via breakage of one of the N–O bonds, resulting in N₂O that contains a 1:1 ratio of NH₄⁺:NO₂⁻. With a precursor such as hyponitrite, equal formation of ⁴⁵N₂O^α and ⁴⁵N₂O^β could be achieved with non-selective N–O bond breakage.

These findings of equal ⁴⁵N₂O production have important implications for the natural abundance δ(¹⁵N^{sp}) of N₂O produced by the hybrid N₂O process. Assuming that hybrid N₂O production proceeds through a symmetrical intermediate in which NH₄⁺ and NO₂⁻ are paired in a 1:1 ratio, we can model δ(¹⁵N^{sp}) as:

$$\delta(^{15}\text{N}^{\text{sp}}) = \delta(^{15}\text{N}^{\alpha}) - \delta(^{15}\text{N}^{\beta})$$

$$= [f\delta(^{15}\text{N} - \text{NO}_2^-) + (1 - f)\delta(^{15}\text{N} - \text{NH}_4^+)] - [(1 - f)\delta(^{15}\text{N} - \text{NO}_2^-) + f\delta(^{15}\text{N} - \text{NH}_4^+) - \varepsilon] \quad (24)$$

where *f* is the proportion of the α nitrogen derived from NO₂⁻ and the proportion of the β nitrogen derived from NH₄⁺, and ε is the fractionation factor associated with N^β–O bond breakage. If *f* ≠ 1/2, hybrid δ(¹⁵N^{sp}) retains a dependence on the δ(¹⁵N) of the substrates – or more accurately, the difference in δ(¹⁵N) of the two substrates; if the δ(¹⁵N) of the substrates is equal, it will cancel out regardless of *f*. If δ(¹⁵N–NH₄⁺) > δ(¹⁵N–NO₂⁻), as is generally the case in the secondary nitrite maximum (Buchwald et al., 2015; Casciotti, 2016), then low values of *f* should produce high hybrid δ(¹⁵N^{sp}), and high values of *f* should produce low hybrid δ(¹⁵N^{sp}) (Fig. 10). If, however, *f* = 1/2, as was the case for most experimental depths in this study, hybrid δ(¹⁵N^{sp}) should depend only on ε and not the isotopic composition of each substrate. This means that a δ(¹⁵N^{sp}) endmember could potentially be established for hybrid N₂O production, even though hybrid N₂O production draws from different substrate pools. More studies are needed to determine the δ(¹⁵N^{sp}) of N₂O produced by ammonia-oxidizing archaea under a range of conditions.

Specific comments:

L80: Actual definition of delta values is

(R_{sample}/R_{standard}–1)

factor 1000 is just due to expression in permil notation, should be omitted in the definition
We removed the factor of 1000 from the definition.

The isotopic content of the individual nitrogen and oxygen atoms in the N₂O molecule are expressed in delta notation, defined as δ(¹⁵N) or δ(¹⁸O) = (R_{sample}/R_{standard}–1), where R_{standard} for

$\delta(^{15}\text{N})$ and $\delta(^{18}\text{O})$ are the ratios $^{15}\text{N}/^{14}\text{N}$ of air and $^{18}\text{O}/^{16}\text{O}$ of Vienna Standard Mean Ocean Water (VSMOW), respectively (Kim and Craig, 1990; Rahn and Wahlen, 2000; Toyoda and Yoshida, 1999).

L 151: 2%-92% - that wide range? is this correct?

This is correct. We added 1 μM $^{15}\text{N}\text{-NO}_3^-$ to all of our experimental depths, regardless of the ambient NO_3^- concentration, resulting in a wide range of atom fractions due to the wide range of ambient NO_3^- concentrations. At depths where ambient NO_3^- is high, however, and thus the atom fraction is low, the rate of N_2O production from NO_3^- is high enough that we still get a detectable signal in $^{45}\text{N}_2\text{O}$ and $^{46}\text{N}_2\text{O}$ (see Figures 4 and 5).

L194: It should be described more precisely how much was added, depending on the concentration and enrichment level? I understand this was just a dilution procedure for mineral nitrogen isotope measurements? Or also for N_2O measurements? It is a bit misleading because this chapter title is N_2O isotopocule measurements... so I am not sure if my understanding is correct. Or you have diluted mineral nitrogen forms in your experiment to dilute your produced N_2O in the headspace? Why not to dilute the N_2O sample with any technical N_2O gas to get respective dilutions?

The first paragraph of Section 2.4 describes the sample preparation procedure, immediately prior to mass spec analysis of liquid samples for nitrous oxide isotopocules. Since we run liquid samples on the purge-and-trap system (see below), we need to protect the purge-and-trap system from highly ^{15}N -enriched NH_4^+ , NO_2^- , and NO_3^- dissolved in the sample. To accomplish this, 100 μL of $^{14}\text{NH}_4\text{Cl}$, $\text{Na}^{14}\text{NO}_2$, or K^{14}NO_3 carrier was added to each sample a final concentration of 54 μM , 262 μM , or 27 μM , respectively, to bring ^{15}N tracer levels below 5000 ‰. We have clarified the above in the text.

Two steps were taken to prepare incubation samples for N_2O isotopocule analysis immediately prior to measurement. First, a 5 mL aliquot was removed from each sample by syringe and replaced with He gas. These aliquots were refrigerated until analysis for $[\text{NO}_2^-]$ and $[\text{NH}_4^+]$ to check tracer and carrier additions, as mentioned above. After this aliquot was removed, 100 μL of $^{14}\text{NH}_4\text{Cl}$, $\text{Na}^{14}\text{NO}_2$, or K^{14}NO_3 carrier was added to each sample a final concentration of 54 μM , 262 μM , or 27 μM , respectively, to bring ^{15}N tracer levels below 5000‰. Note that these carrier additions were different from the ^{14}N carrier added to each incubation alongside ^{15}N tracer; the purpose of the later carrier additions was to prevent exposure of the IRMS system to highly ^{15}N -enriched substrates.

section 2.4: Actually you do not say how you finally collect your gaseous N_2O samples - which volume, which containers, which procedure? Were the N_2O samples collected once only from each bottle or regularly in some time intervals?

We apologize for any confusion here. The purge-and-trap system completely extracts the dissolved N_2O from the sample (incubation) bottle and is described in greater detail in McIlvin and Casciotti (2010). So, one bottle = one sample. Time series are constructed by sacrificing triplicate bottles over a time course, rather than resampling the incubation bottles over time. This time series approach is now stated explicitly in the methods section.
Time series were constructed by sacrificing triplicate bottles over a time course, rather than resampling the incubation bottles over time.

We describe how liquid samples were collected for incubation in section 2.2, “sample collection.”

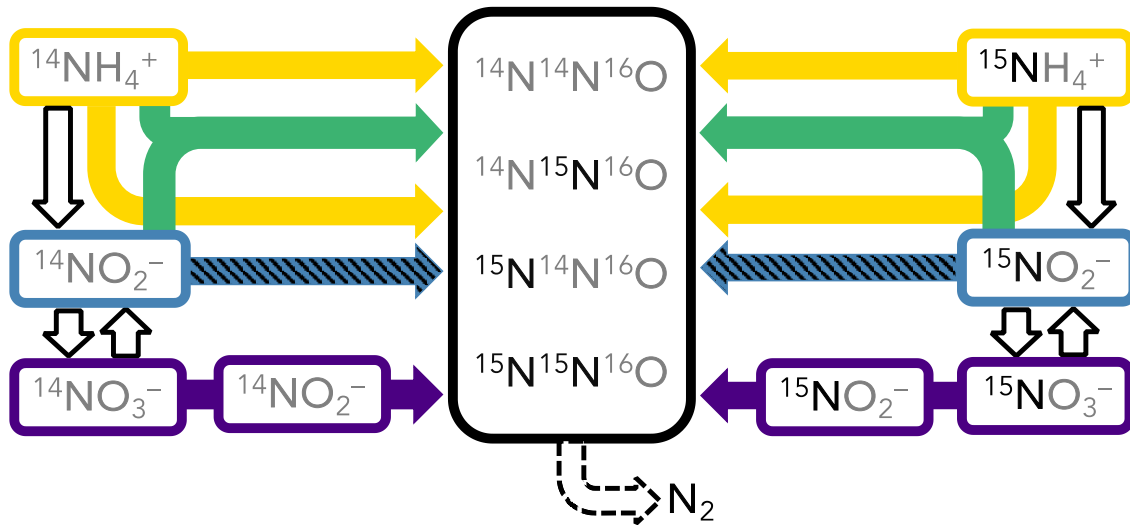
Equation 3: what value was assumed for D17O?

$\Delta(^{17}\text{O})$ was assumed to be 0. We have added this to the text.

Here, $\Delta(^{17}\text{O})$ was assumed to be equal to 0.

Figure 2: should the yellow arrow between NH_4 and NO_2^- go in both directions? since this represents formation of hybrid N_2O with cellular NO_2^- , right?

We added an arrow representing hybrid N_2O with cellular NO_2^- . The vertical arrow was between NH_4^+ and NO_2^- was a bit confusing since it did not represent an N_2O production processes, only NH_4^+ oxidation to NO_2^- . We made the vertical arrows colorless to indicate that they are not N_2O production processes.



Pathway name	Includes N_2O production from...	Corresponding process in Wan et al. (2023)
Production from solely NH_4^+	Hydroxylamine oxidation	Pathway 1
	Hybrid production using cellular NO_2^-	Pathway 2
	Nitrifier–denitrification using cellular NO_2^-	N/A
Hybrid production	Hybrid production using extracellular NO_2^-	Pathway 3
Production from NO_2^-	Denitrification or nitrifier–denitrification using extracellular NO_2^-	N/A
Production from NO_3^-	Denitrification using cellular NO_2^-	N/A

Figure 2. Schematic of the forward–running model used to solve for rates of N_2O production. Horizontal arrows represent processes whose rates are solved for, while vertical arrows represent processes whose rates are prescribed based on our experimental results. The model solves for 2nd–order rate constants for four N_2O –producing processes: 1) production from solely NH_4^+ (yellow horizontal arrows), which includes N_2O from hydroxylamine oxidation (Wan et al., 2023 Pathway 1), hybrid production using cellular NO_2^- (Wan et al., 2023 Pathway 2), and nitrifier–denitrification using cellular NO_2^- ; 2) hybrid production using NH_4^+ and extracellular NO_2^- (green arrows, Wan et al., 2023 Pathway 3); 3) production from NO_2^- , i.e. denitrification or nitrifier–denitrification using extracellular NO_2^- (blue hatched horizontal arrows); and 4) production from NO_3^- , i.e. denitrification

or nitrifier–denitrification using cellular NO_2^- (indigo horizontal arrows). The model also solves for f , the proportion of N^α derived from NO_2^- during hybrid N_2O production. NH_3 oxidation (yellow vertical arrows), NO_2^- oxidation (blue hatched vertical arrows), and NO_3^- reduction to NO_2^- (indigo vertical arrows) are modeled as first–order rates to account for ^{15}N transfer between substrate pools, as described in the main text. Finally, N_2O consumption (black dashed arrow) is modeled as first–order to N_2O . It is assumed that while the distribution of ^{15}N in each tracer experiment at a given station and depth is different, the overall rates and mechanisms of N_2O production are the same regardless of which substrate is labeled. The model is optimized against the observed $^{46}\text{N}_2\text{O}$, $^{45}\text{N}_2\text{O}^\alpha$, $^{45}\text{N}_2\text{O}^\beta$, and $^{44}\text{N}_2\text{O}$ at each timepoint in each tracer experiment (black box).

Equation 18: I think this definition, with some explanation why this is possible should appear in methods section 2.6 This does not fit in results section. Same with Eq. 19

We respectfully disagree. Section 2.6 describes the modeling framework, and the model does not use equations (18) and (19). Actually, the modeling framework is a much more nuanced way of estimating the rates of hybrid N_2O formation than simply using eqns. (18) and (19). Eqns. (18) and (19) are just a way of showing that hybrid N_2O production is indeed occurring in our experiments, which we do in section 3.3.

L 550: Why there is such large difference in NH_3 oxidation with different studies? - it should be discussed - is this due to different analytical approaches?

There are several factors that may have contributed to Travis et al. (2023) measuring higher rates of ammonia oxidation than our study or that of Frey et al. (2023). The incubations in Travis et al. (2023) were performed at different depths than ours, so they likely captured different microbial communities, different light levels, different chemical conditions (nitrate, dissolved oxygen, etc.). This is further exaggerated by the fact that the oxycline was moving up and down during the course of our occupation of PS3 (as indicated by oxygen profiles captured by an Argo float near our sampling stations during the time of our cruise, Figure S4 in Sun et al., 2021), so even experiments performed at the same depth on different days would likely sample different biogeochemical conditions. Nitrification rates tend to show a very sharp subsurface maximum (the feature Travis et al focused on) and the resolution of the depth profiles in our study was not optimized to “catch” it. Finally, the incubations performed in Travis et al. (2023) were fully aerobic, whereas ours were generally low-oxygen and gas-tight. For example, the dissolved oxygen in our incubation with the highest rates of ammonia oxidation was 2 μM (see tables S1 and S2).

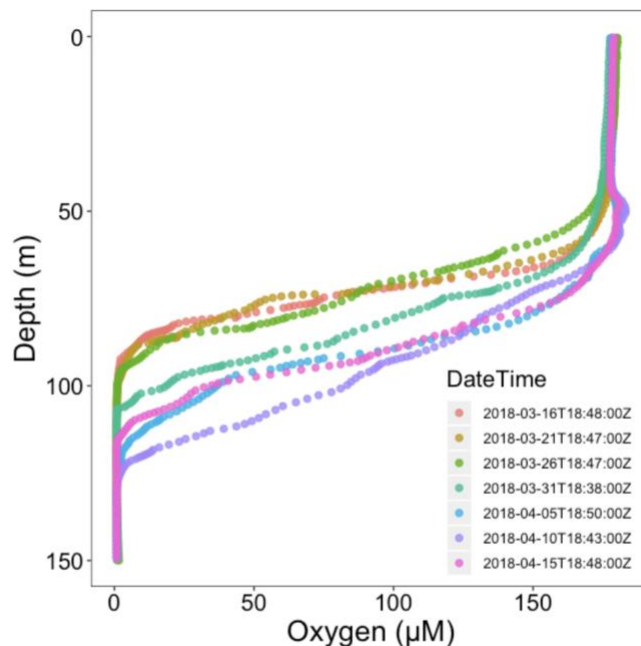


Figure S4. O₂ profiles based on one Argo float at a station (13.1 N, 108.4 W) between our sampling stations PS2 and PS3 in the ETNP OMZ. These data were collected in the same month that our samples were collected. Color indicates the date and time of data collection. The 20 m interval (100–120 m) varied from nearly 100 μM to below detection within two weeks.

We also needed to make a correction: the highest rate of ammonia oxidation measured by Travis et al. (2023) was actually 90 ± 2 nM/day, not 48.7 nM/day.

NH₃ oxidation rates in this study were smaller than those measured on the same cruise by Travis et al. (2023), who measured NH₃ oxidation rates as high as 90 ± 2 nM/day in fully oxygenated incubations at station PS3.

L 600: why, which process can be responsible for this? Very important observation! You could give more details to these points - which processes dominated there, what was the N₂O flux (rather high or low) or how it is possible to interpret these data?

Please see comments in response to L 613.

L 613: But in the first and second paragraph in this section 4.2 you showed that the values originating from NO₂ and NH₄ are mixed and finally the formed N₂O has randomly situated 15N atoms from NO₂ and NH₄

I see, below the Eq (24) you explain, in most cases it is equally distributed but in some it is not. But why? The reader is a bit lost here

In the second paragraph you described very precisely how the hybrid formation may function and why we get equal distribution, and this is very convincing. So, the few cases with f unequal

0.5 must be due to some other process, some different mechanism? I understand this is rather an exception than a rule for hybrid formation – but you define this as a rule in Eq.24 (and then repeat this as final conclusion).

This is very important to describe this correctly here because for NA studies we do not know f , hence your conclusions here will be crucial for d15N-SP interpretations in NA studies.

Thank you for these comments. We revised the discussion in section 4.2 to reflect the fact that the majority of our experiments have equal formation of $^{45}\text{N}_2\text{O}^\alpha$ and $^{45}\text{N}_2\text{O}^\beta$ and f within error of 0.5. This is actually a very important finding for the interpretation of natural abundance N_2O isotopocules because it implies that hybrid N_2O would indeed have a constant $\delta(^{15}\text{N}^{\text{sp}})$, despite being derived from two different sources. We revised section 4.2, the conclusions, and the abstract to reflect the equal formation of $^{45}\text{N}_2\text{O}^\alpha$ and $^{45}\text{N}_2\text{O}^\beta$ seen in most of our experiments and the implications of f being equal to 0.5.

4.2 Pathways of hybrid N_2O production and implications for hybrid $\delta(^{15}\text{N}^{\text{sp}})$

Hybrid N_2O production peaked in the same depths as NH_3 oxidation (Fig. 6c, g, k), which were also the depths at which ammonia-oxidizing archaea were most abundant (Frey et al., 2023), consistent with N_2O production associated with ammonia-oxidizing archaea. At most stations and depths, the production of $^{45}\text{N}_2\text{O}^\alpha$ and $^{45}\text{N}_2\text{O}^\beta$ in both the $^{15}\text{N}\text{-NO}_2^-$ and $^{15}\text{N}\text{-NH}_4^+$ experiments were roughly equal. From this we conclude that during hybrid formation, N^α and N^β each retained nitrogen atoms derived from both NH_4^+ and NO_2^- . The equal formation of $^{45}\text{N}_2\text{O}^\alpha$ and $^{45}\text{N}_2\text{O}^\beta$ led to values of f within error of 0.5 in most of our experiments (Table S4), and the mean value of f across all stations and depths was 0.5 ± 0.2 . This means that during hybrid N_2O production, half of the N^α atoms were derived from NO_2^- , and half were derived from NH_4^+ (likewise for N^β).

Although our data do not allow us to comment directly on the enzymatic machinery of hybrid N_2O formation, our data can be used to theorize hypothetical pathways for hybrid N_2O production. Firstly, we see much higher rates of hybrid production using ambient NO_2^- (Pathway 3 in Wan et al., 2023) than hybrid production using cellular NO_2^- (Pathway 2 in Wan et al., 2023). Again, this agrees with the results of Wan et al. (2023), who see higher rates of hybrid formation from extracellular NO_2^- within the range of $[\text{N}^{15}\text{-NH}_4^+]/[\text{NO}_2^-]$ covered by our experiments. In our model, hybrid N_2O production is operationally defined as a 1:1 combination of N derived from NH_4^+ and NO_2^- , which is generally consistent with previous work (Stieglmeier et al., 2014). Any combination of N derived from NO_2^- with a second N derived from NO_2^- would be included in the modeled quantity of N_2O production from NO_2^- ; likewise, any combination of N derived from NH_4^+ with a second N derived from NH_4^+ would be included in the N_2O production from solely NH_4^+ . The question, then, is what reaction would be specific enough to have one N derived from each substrate, but not specific enough to govern ^{15}N placement in the resulting N_2O ? One such reaction could be the combination of NH_4^+ and NO_2^- to form a symmetrical intermediate such as hyponitrite (HONNOH or $^-\text{ONNO}^-$ in its deprotonated form), which reacts to form N_2O via breakage of one of the $\text{N}\text{-O}$ bonds, resulting in N_2O that contains a 1:1 ratio of $\text{NH}_4^+:\text{NO}_2^-$. With a precursor such as hyponitrite, equal formation of $^{45}\text{N}_2\text{O}^\alpha$ and $^{45}\text{N}_2\text{O}^\beta$ could be achieved with non-selective $\text{N}\text{-O}$ bond breakage.

These findings of equal $^{45}\text{N}_2\text{O}$ production have important implications for the natural abundance $\delta(^{15}\text{N}^{\text{sp}})$ of N_2O produced by the hybrid N_2O process. Assuming that hybrid N_2O production proceeds through a symmetrical intermediate in which NH_4^+ and NO_2^- are paired in a 1:1 ratio, we can model $\delta(^{15}\text{N}^{\text{sp}})$ as:

$$\begin{aligned} \delta(^{15}\text{N}^{\text{sp}}) &= \delta(^{15}\text{N}^\alpha) - \delta(^{15}\text{N}^\beta) \\ &= [f\delta(^{15}\text{N} - \text{NO}_2^-) + (1 - f)\delta(^{15}\text{N} - \text{NH}_4^+)] - [(1 - f)\delta(^{15}\text{N} - \text{NO}_2^-) + f\delta(^{15}\text{N} - \text{NH}_4^+) - \varepsilon] \quad (24) \end{aligned}$$

where f is the proportion of the α nitrogen derived from NO_2^- and the proportion of the β nitrogen derived from NH_4^+ , and ε is the fractionation factor associated with $\text{N}^\beta\text{-O}$ bond breakage. If $f \neq 1/2$, hybrid $\delta(^{15}\text{N}^{\text{sp}})$ retains a dependence on the $\delta(^{15}\text{N})$ of the substrates – or more accurately, the difference in $\delta(^{15}\text{N})$ of the two substrates; if the $\delta(^{15}\text{N})$ of the substrates is equal, it will cancel out regardless of f . If $\delta(^{15}\text{N}\text{-NH}_4^+) > \delta(^{15}\text{N}\text{-NO}_2^-)$, as is generally the case in the secondary nitrite maximum (Buchwald et al., 2015; Casciotti, 2016), then low values of f should produce high hybrid $\delta(^{15}\text{N}^{\text{sp}})$, and high values of f should produce low hybrid $\delta(^{15}\text{N}^{\text{sp}})$ (Fig. 10). If, however, $f = 1/2$, as was the case for most experimental depths in this study, hybrid $\delta(^{15}\text{N}^{\text{sp}})$ should depend only on ε and not the isotopic composition of each substrate. This means that a $\delta(^{15}\text{N}^{\text{sp}})$ endmember could potentially be established for hybrid N_2O production, even though hybrid N_2O production draws from different substrate pools. More studies are needed to determine the $\delta(^{15}\text{N}^{\text{sp}})$ of N_2O produced by ammonia-oxidizing archaea under a range of conditions.

L 630: ok, but maybe you can sum up what were the conditions for the samples with f unequal 0.5 in your studies

I believe that it is rather not the hybrid process that behaves sometimes like this and sometimes the other way but rather admixture of some other processes, or the issue with the usage of cellular and extracellular NO_2^- . What about possible fungal co-denitrification that may show different mechanism?

I think you have so much data that maybe some hypotheses can be made?

The experiments with unequal $^{45}\text{N}_2\text{O}^\alpha$ and $^{45}\text{N}_2\text{O}^\beta$ formation spanned a range of oxygen concentrations, depths, and substrate concentrations, and no clear patterns emerged. We do note that significant relationships emerged between f and ambient $[\text{O}_2]$ ($R^2 = 0.84$, $p < 0.001$; Fig. S12a) and potential density anomaly (σ_θ) ($R^2 = 0.72$, $p < 0.001$; Fig. S12b), although both relationships exhibited a large amount of scatter. These oxygen and potential density gradients may be proxies for changing archaeal community compositions at different depths in the water column, which may exhibit different patterns of incorporation of NO_2^- -derived N and NH_4^+ -derived N into N^α and N^β . We now note this in the text.

Thanks for the suggestion that we may have sampled a different “hybrid” process at these depths, such as fungal co-denitrification (Shoun et al., 2012), which may proceed via a

different pathway from archaeal hybrid N₂O production. We added this alternative to the text.

*The unequal production of ⁴⁵N₂O^α and ⁴⁵N₂O^β observed at certain depths led to values of *f* significantly different from 0.5 (Table S4). At these depths, N^α retained a different proportion of nitrogen derived from NO₂⁻ and NH₄⁺ than N^β, causing ⁴⁵N₂O^α and ⁴⁵N₂O^β to diverge. The depths with *f* ≠ 0.5 anchored significant relationships between *f* and ambient [O₂] (R² = 0.84, *p* < 0.001; Fig. S10a) and potential density anomaly (σ_θ) (R² = 0.72, *p* < 0.001; Fig. S10b). The oxygen and potential density gradients may be proxies for changing archaeal community compositions at different depths in the water column, which may exhibit different patterns of incorporation of NO₂⁻-derived N and NH₄⁺-derived N into N^α and N^β. It is also possible that we sampled a different “hybrid” N₂O-producing process at these depths, such as fungal co-denitrification (Shoun et al., 2012), which may proceed via a different pathway from archaeal hybrid N₂O production.*

L 703: Have you observed any activity, any N₂O production in HgCl₂ poisoned treatments? Would be interesting to report what was the "background" N₂O production, since in some studies it appears quite high.

Was this in the expected range of abiotic N₂O production?

We agree with the reviewer that there is a concern about abiotic reactions between NO₂⁻ and HgCl₂. In our ¹⁵N-NO₂⁻ experiments, the t₀ samples did not have δ(¹⁵N-N₂O) or δ(¹⁸O-N₂O) outside of the natural abundance range, which would have indicated an abiotic reaction between the ¹⁵N-NO₂⁻ tracer and HgCl₂ e.g., during storage of the samples prior to analysis. In comparison, we do see some elevated δ(¹⁵N-NO_x) in these samples (Figure S2), indicating that the sulfamic acid treatment may have converted some ¹⁵N-NO₂⁻ to ¹⁵N-NO₃⁻, and/or that there was ¹⁵N-NO₃⁻ contamination in our ¹⁵N-NO₂⁻ tracer. That is why it is important to measure t₀'s in case an abiotic reaction should shift the baseline and it is necessary to account for this shift, as we have done.

L 724: But this conclusion is not supported by the previous sentence. From the mechanism you describe it is expected that the alpha and beta positions are independent of the substrate origin.

I do not agree with this conclusion since MOST of your samples do not support this, only in few cases you observed differences in alpha and beta position, so rather the opposite conclusion should be given here, with an indication that there are also some exceptions, with not fully understood mechanism (in my opinion resulting from admixture of processes which has not been taken into consideration - e.g. fungal co-denitrification - which you admit in section 4.6, that fungal N₂O can be an important source and it is not included in your model). You have actually concluded this at the end of your section 4.2 properly. You cannot simplify this into different direction in the conclusions because people will mostly read only conclusions, and this is very important point impacting the interpretations of natural abundance N₂O isotopocule studies very much.

We revised the conclusions to reflect the fact that we see equal formation of ⁴⁵N₂O^α and ⁴⁵N₂O^β in most of our experiments, and thus that hybrid N₂O is *not* likely to have a variable

$\delta(^{15}\text{N}^{\text{sp}})$. This is an equally strong conclusion because it implies that it may be possible to define a $\delta(^{15}\text{N}^{\text{sp}})$ endmember for hybrid N_2O formation.

5. Conclusions

We applied N_2O isotopocule measurements to ^{15}N tracer incubations to measure N_2O production rates and mechanisms in the ETNP. We found that N_2O production rates peaked at the oxic–anoxic interface above the ODZ, with the highest rates of N_2O production from NO_3^- . Hybrid N_2O production peaked in both the shallow and deep oxyclines, where NH_3 oxidation was also active, and exhibited yields as high as 21% of ammonia oxidation.

Based on the equal production of $^{45}\text{N}_2\text{O}^\alpha$ and $^{45}\text{N}_2\text{O}^\beta$ in the vast majority of our experiments, we posit a two–step process for hybrid N_2O production involving an initial bond–forming step that draws nitrogen atoms from each substrate to form a symmetric intermediate, and a second bond–breaking step that breaks an N–O bond in the symmetric intermediate to form N_2O . From this, we infer that hybrid N_2O production likely has a consistent $\delta(^{15}\text{N}^{\text{sp}})$, despite drawing from two distinct substrate pools. This has important implications for the interpretation of natural abundance isotopocule measurements, since it implies that it may be possible to define a $\delta(^{15}\text{N}^{\text{sp}})$ endmember for hybrid N_2O formation. More culture experiments are needed to quantify the $\delta(^{15}\text{N}^{\text{sp}})$ of N_2O produced by ammonia–oxidizing archaea under different temperatures, oxygen levels, and ratios of $\text{NH}_4^+:\text{NO}_2^-$.

733: These observations can be also due to fungal activity since fungal species usually tolerate higher oxygen levels than bacteria.

Thank you for pointing this out. We added fungal denitrification as a potential explanation for some of the N_2O production from denitrification at higher oxygen levels than expected, both in the conclusions and in section 4.4, “Oxygen dependence of N_2O production rates and yields”.

Most surprising were the significant rates of N_2O production via denitrification at $[\text{O}_2] > 3 \mu\text{M}$ (Fig. 8g–h), which has previously been suggested as the threshold above which denitrification ceases (Dalsgaard et al., 2014). These observations are particularly evident in the plots of N_2O production from NO_3^- vs. incubation $[\text{O}_2]$ (Fig. 8h), where positive, significant rates of N_2O production from NO_3^- were evident in incubations containing $[\text{O}_2]$ as high as $19.2 \pm 0.8 \mu\text{M}$ (PS2 Deep ODZ Core experiment). One explanation for N_2O production via denitrification at such high levels of ambient dissolved oxygen is particle–associated denitrification (Bianchi et al., 2018; Smriga et al., 2021; Wan et al., 2023a). Fungal denitrification may also have contributed to these fluxes, since denitrifying fungi can tolerate a higher level of oxygen than their bacterial counterparts.

Reviewer 3

The authors present an impressively thorough analysis of N₂O isotope systematics from a field study in the oxygen deficient zone of the eastern tropical north Pacific (ETNP) – a region well studied for its redox active nitrogen cycle. Through a suite of ¹⁵N labeling experiments and the leveraging of those results, the paper lays out a complex yet compelling argument for the ecological distribution of various pathways of N₂O production. Taking the isotopic scrutiny to the next level, the paper presents a powerful and novel analytical model that leverages both the relative formation of singly labeled (⁴⁵N₂O) and doubly labeled (⁴⁶N₂O) as well as the site-specific labeling of the inner (alpha) and outer (beta) N atoms across all experiments (e.g., ¹⁵N labeled NH₄⁺, NO₂⁻ or NO₃⁻) to solve for relative contribution of N₂O formation pathways. To my knowledge, such a sophisticated analysis has not been braved – and the authors should be commended for it.

The authors also use their results to evaluate the O₂ sensitivities of each of the formation pathways under these field incubation conditions, tying the results to both in situ O₂ and incubation levels of O₂ (which sometimes differed from in situ). These results show that adopted thresholds for N₂O production by denitrification (for example) may not be as hard and fast as previously thought. The data provide quantitative relationships from which models can be built for estimating wider patterns in N₂O production.

Especially unique and thought-provoking was the model analysis interrogating the possible impact on natural abundance site-preference compositions in N₂O as arising from hybrid formation – especially the proposed involvement of a symmetric intermediate. I very much enjoyed Section 4.2 which carefully walks the reader through the logic of the analysis and argues for the hybrid pathway involving formation of a symmetric intermediate (such as hyponitrite). Equation 24 demonstrates how, with a symmetric intermediate (and a 50/50 contribution of NH₄⁺ and NO₂⁻ precursors) – the actual composition of the precursors does not impact site preference. However, if this 50/50 proportion varies (as they observe in some incubations) – then this assumption falls apart – and could in fact explain or demonstrate that the site preference values for hybrid N₂O formation may vary under differing ambient conditions. While exceptionally nuanced, I found the arguments laid out in this section to offer real strides forward in our collective understanding.

I also found particularly useful the demonstration of how go about combining probabilistic analysis of N₂O formation (e.g., stochastic distribution of ¹⁵R between alpha and beta positions) with the ¹⁵N labeling exercise (where an excess of doubly labeled N₂O (15-15-16) may arise depending on formation pathways). Introduction of this ‘excess’ term allows for the application of site-specific composition to determine N atom sources under ¹⁵N labeling circumstances. To my knowledge, this approach has not been leveraged previously – and thus the manuscript contains a wealth of valuable methodological information – which I found laid out very clearly. Thus, the paper should also stand as a useful model for work beyond N₂O dynamics in ODZs – and could provide a model for application to a range of other systems.

Overall, because of the complex nature of the work - this paper is a beast to get through. That being said – it is excellently written and offers a wealth of value for really pulling apart the

complexity of environmental N₂O formation. I provide some minor editorial comments below which hopefully help to highlight some areas that could be clarified. I recommend publication.

We are sincerely grateful for this positive and thorough evaluation of our work. Thank you for taking the time to work through the many aspects of this paper.

Specific Comments:

There is a lot of complex discussion of N₂O isotope systematics – which are notoriously challenging to understand. I can see that the authors are very careful to be clear in explaining most things and using careful wording for helping the readers follow the logic.

What were isotope effects used for NH₄⁺ oxidation, etc.? Table? Would variation of these values (for example) impact the error estimates as mentioned in L350-352?

We added a supplementary table (now Table S3) of the isotope effects used in the model for NH₄⁺ oxidation, NO₂⁻ oxidation, NO₃⁻ reduction, and N₂O reduction. Since we're dealing with tracer-level ¹⁵N, though, natural abundance-level isotope effects are unlikely to affect the model results. No isotope effects were applied to N₂O formation.

Table S3. Fractionation factors used the time-dependent numerical model.

Process	¹⁵ ε ^{bulk} (‰)	¹⁵ ε ^α (‰)	¹⁵ ε ^β (‰)	Reference
NH ₄ ⁺ oxidation	22.0			Santoro and Casciotti, 2011
NO ₂ ⁻ oxidation	-15.0			Casciotti, 2009
NO ₃ ⁻ reduction to NO ₂ ⁻	5.0			Granger et al., 2008
N ₂ O reduction to N ₂		11.8	0.0	Kelly et al., 2021

While I recognize here a nomenclature used for isotope ratios (e.g., “δ(¹⁵N)”) has been adopted to be in line with some recent protocols, I find the use of the extra set of parentheses extremely distracting, unnecessary, and confusing. While I'm sure that the adoption of such conventions was intended to help clarify, the addition of more symbols into these terms does not help the reader and frankly muddies the message. I may very well be a minority here, but simply don't see the logic in these new conventions (especially in the context of N₂O which is already complex enough). I see zero value in adopting the new nomenclature, and though probably futile, would suggest the authors stick to the nomenclature that has been in use for decades (e.g., δ¹⁵N).

The justification for writing δ values with parentheses, e.g., δ(¹⁵N), is that δ is the quantity symbol and “¹⁵N” is the label. I started using this notation in Kelly et al. (2023) in order to reflect the recommendations in the latest SI Brochure (<https://www.bipm.org/en/publications/si-brochure/>) and I continue its use here for consistency and semantic precision. I understand that this is a change from the conventions in the field and is likely to be unpopular, but perhaps the notation will become less confusing if it is more widely adopted.

The paragraphs starting on Line 610, together with Equation 24 and Figure 8 worked to convince me that when the proportion of NO_2^- and NH_4^+ to hybrid N_2O formation is equal (and the intermediate is a symmetric molecule), then the actual ^{15}N content (or $\delta^{15}\text{N}$ value) of those substrates does not play a role in the emergent site preference value. Why then on line 725 in the conclusion – do the authors state that these values do matter (even if 1:1 contribution)? Is it not true that the hypothetically variable site preference values from hybrid N_2O formation actually emerge from variations in the 50/50 (or 1:1) contribution – and that only in those cases will the values of the substrates play into the site preference of the product N_2O (as in Figure 8)? Please clarify.

Thank you for this comment. When the contributions of NO_2^- and NH_4^+ to each N position are equal, hybrid site preference doesn't depend on the isotopic composition of either substrate. You could hypothetically have N_2O containing a 1:1 ratio of NO_2^- and NH_4^+ , but with N^α always derived from NO_2^- ($f=1$), and in this case site preference would depend strongly on the isotopic composition of each substrate. But in most of our experiments, N^α is equally derived from NO_2^- and NH_4^+ , which would imply that hybrid site preference does not vary. This means that it may even be possible to identify an isotopic endmember for hybrid N_2O production, which would be very useful to the natural abundance N_2O isotopocule community. We have revised the discussion and throughout the paper to reflect this majority case. This is an important clarification of the results, so we are grateful to you (and the other reviewers) for pointing this out.

4.2 Pathways of hybrid N_2O production and implications for hybrid $\delta(^{15}\text{N}^{\text{sp}})$

Hybrid N_2O production peaked in the same depths as NH_3 oxidation (Fig. 6c, g, k), which were also the depths at which ammonia-oxidizing archaea were most abundant (Frey et al., 2023), consistent with N_2O production associated with ammonia-oxidizing archaea. At most stations and depths, the production of $^{45}\text{N}_2\text{O}^\alpha$ and $^{45}\text{N}_2\text{O}^\beta$ in both the $^{15}\text{N}\text{-NO}_2^-$ and $^{15}\text{N}\text{-NH}_4^+$ experiments were roughly equal. From this we conclude that during hybrid formation, N^α and N^β each retained nitrogen atoms derived from both NH_4^+ and NO_2^- . The equal formation of $^{45}\text{N}_2\text{O}^\alpha$ and $^{45}\text{N}_2\text{O}^\beta$ led to values of f within error of 0.5 in most of our experiments (Table S4), and the mean value of f across all stations and depths was 0.5 ± 0.2 . This means that during hybrid N_2O production, half of the N^α atoms were derived from NO_2^- , and half were derived from NH_4^+ (likewise for N^β).

Although our data do not allow us to comment directly on the enzymatic machinery of hybrid N_2O formation, our data can be used to theorize hypothetical pathways for hybrid N_2O production. Firstly, we see much higher rates of hybrid production using ambient NO_2^- (Pathway 3 in Wan et al., 2023) than hybrid production using cellular NO_2^- (Pathway 2 in Wan et al., 2023). Again, this agrees with the results of Wan et al. (2023), who see higher rates of hybrid formation from extracellular NO_2^- within the range of $[^{15}\text{N}\text{-NH}_4^+]/[\text{NO}_2^-]$ covered by our experiments. In our model, hybrid N_2O production is operationally defined as a 1:1 combination of N derived from NH_4^+ and NO_2^- , which is generally consistent with previous work (Stieglmeier et al., 2014). Any combination of N derived from NO_2^- with a second N derived from NO_2^- would be included in the modeled quantity of N_2O production from NO_2^- ; likewise, any combination of N derived from NH_4^+ with a second N derived from NH_4^+ would be included in the N_2O production from solely NH_4^+ . The question, then, is what reaction would be specific enough to

have one N derived from each substrate, but not specific enough to govern ^{15}N placement in the resulting N_2O ? One such reaction could be the combination of NH_4^+ and NO_2^- to form a symmetrical intermediate such as hyponitrite (HONNOH or $^-\text{ONNO}^-$ in its deprotonated form), which reacts to form N_2O via breakage of one of the N–O bonds, resulting in N_2O that contains a 1:1 ratio of $\text{NH}_4^+:\text{NO}_2^-$. With a precursor such as hyponitrite, equal formation of $^{45}\text{N}_2\text{O}^\alpha$ and $^{45}\text{N}_2\text{O}^\beta$ could be achieved with non-selective N–O bond breakage.

These findings of equal $^{45}\text{N}_2\text{O}$ production have important implications for the natural abundance $\delta(^{15}\text{N}^{\text{sp}})$ of N_2O produced by the hybrid N_2O process. Assuming that hybrid N_2O production proceeds through a symmetrical intermediate in which NH_4^+ and NO_2^- are paired in a 1:1 ratio, we can model $\delta(^{15}\text{N}^{\text{sp}})$ as:

$$\begin{aligned} \delta(^{15}\text{N}^{\text{sp}}) &= \delta(^{15}\text{N}^\alpha) - \delta(^{15}\text{N}^\beta) \\ &= [f\delta(^{15}\text{N} - \text{NO}_2^-) + (1 - f)\delta(^{15}\text{N} - \text{NH}_4^+)] - [(1 - f)\delta(^{15}\text{N} - \text{NO}_2^-) + f\delta(^{15}\text{N} - \text{NH}_4^+) - \varepsilon] \quad (24) \end{aligned}$$

where f is the proportion of the α nitrogen derived from NO_2^- and the proportion of the β nitrogen derived from NH_4^+ , and ε is the fractionation factor associated with $\text{N}^\beta\text{--O}$ bond breakage. If $f \neq 1/2$, hybrid $\delta(^{15}\text{N}^{\text{sp}})$ retains a dependence on the $\delta(^{15}\text{N})$ of the substrates – or more accurately, the difference in $\delta(^{15}\text{N})$ of the two substrates; if the $\delta(^{15}\text{N})$ of the substrates is equal, it will cancel out regardless of f . If $\delta(^{15}\text{N}\text{--}\text{NH}_4^+) > \delta(^{15}\text{N}\text{--}\text{NO}_2^-)$, as is generally the case in the secondary nitrite maximum (Buchwald et al., 2015; Casciotti, 2016), then low values of f should produce high hybrid $\delta(^{15}\text{N}^{\text{sp}})$, and high values of f should produce low hybrid $\delta(^{15}\text{N}^{\text{sp}})$ (Fig. 10). If, however, $f = 1/2$, as was the case for most experimental depths in this study, hybrid $\delta(^{15}\text{N}^{\text{sp}})$ should depend only on ε and not the isotopic composition of each substrate. This means that a $\delta(^{15}\text{N}^{\text{sp}})$ endmember could potentially be established for hybrid N_2O production, even though hybrid N_2O production draws from different substrate pools. More studies are needed to determine the $\delta(^{15}\text{N}^{\text{sp}})$ of N_2O produced by ammonia-oxidizing archaea under a range of conditions.

5. Conclusions

We applied N_2O isotopocule measurements to ^{15}N tracer incubations to measure N_2O production rates and mechanisms in the ETNP. We found that N_2O production rates peaked at the oxic–anoxic interface above the ODZ, with the highest rates of N_2O production from NO_3^- . Hybrid N_2O production peaked in both the shallow and deep oxyclines, where NH_3 oxidation was also active, and exhibited yields as high as 21% of ammonia oxidation.

Based on the equal production of $^{45}\text{N}_2\text{O}^\alpha$ and $^{45}\text{N}_2\text{O}^\beta$ in the vast majority of our experiments, we posit a two-step process for hybrid N_2O production involving an initial bond-forming step that draws nitrogen atoms from each substrate to form a symmetric intermediate, and a second bond-breaking step that breaks an N–O bond in the symmetric intermediate to form N_2O . From this, we infer that hybrid N_2O production likely has a consistent $\delta(^{15}\text{N}^{\text{sp}})$, despite drawing from two distinct substrate pools. This has important implications for the interpretation of natural abundance isotopocule measurements, since it implies that it may be possible to define a $\delta(^{15}\text{N}^{\text{sp}})$ endmember for hybrid N_2O formation. More culture experiments are needed to quantify the

$\delta(^{15}\text{N}^{\text{sp}})$ of N_2O produced by ammonia-oxidizing archaea under different temperatures, oxygen levels, and ratios of $\text{NH}_4^+:\text{NO}_2^-$.

Technical Corrections:

Methods: Perhaps I missed this somewhere. What volume of sample was collected for the N_2O analyses? 160ml serum bottles? Foil bags?

In 2.2, “Sample collection,” we state that “Incubation samples were filled directly from Niskin bottles into 160 mL glass serum bottles (Wheaton) using Tygon tubing. Incubation bottles were overflowed three times before being capped and sealed with no headspace using gray butyl rubber septa (National Scientific) and aluminum crimp seals.” In response to this comment and a similar comment from Reviewer 2, we added a clarification that time series were constructed by sacrificing triplicate bottles over a time course, rather than resampling the incubation bottles over time.

Time series were constructed by sacrificing triplicate bottles over a time course, rather than resampling the incubation bottles over time.

L24: N_2O formatting

Corrected

Using ^{15}N -labeled tracer incubations, we measured the rates of N_2O production from ammonium (NH_4^+), nitrite (NO_2^-), and nitrate (NO_3^-) in the Eastern Tropical North Pacific ODZ, as well as the isotopic labeling of the central (α) and terminal (β) nitrogen atoms of the N_2O molecule.

L25: ‘forward running model’ – unclear what this means... numerical model? Analytical model? Is there some terminology you could use here to help clarify?

Changed to “time-dependent numerical model”.

Implementing the rates of labeled N_2O production in a time-dependent numerical model, we found that N_2O production from NO_3^- dominated at most stations and depths, with rates as high as 1600 ± 200 pM $\text{N}_2\text{O}/\text{day}$.

L 86: instead of ‘unlinked to’ (which seems a little awkward) maybe consider ‘independent from’

Corrected.

In natural abundance studies, $\delta(^{15}\text{N}^{\text{sp}})$ is particularly useful because it exhibits distinct values for different N_2O production processes, independent of the isotopic value of the substrate (Toyoda et al., 2002; Sutka et al., 2003, 2006, 2004; Toyoda et al., 2005; Frame and Casciotti, 2010).

L134: Was the introduction of this background N_2O done as a gas or in dissolved form?

Gas form. Added to the text.

After sparging, 100 μL of 1030 ppm N_2O in He (4 nmol N_2O) in gaseous form was introduced back into each bottle for a final concentration of 26 nM to provide a constant background of N_2O for later isotopic analysis (Fig. S4a).

L148: ... to provide enough total NO_2^- ...

Corrected.

The Na¹⁴NO₂ and ¹⁴NH₄Cl amendments served two purposes: 1) to provide enough total NO₂⁻ for isotopic analysis of ¹⁵NO₂⁻ produced from ¹⁵NH₄⁺, and 2) to minimize isotope dilution of the substrate pool, which can cause underestimation of rates with low substrate additions.

L229: Here referring to the precision being lower, but the standard deviations being higher is a little confusing. Perhaps refer to the precision being ‘poorer’?

Corrected.

The analytical precision was poorer than that in a similar natural abundance dataset (Kelly et al., 2021) due to minor ¹⁵N carry-over in some of the standards analyzed immediately following highly enriched samples.

L245: ...another explanation would be that the ¹⁵NO₂⁻ tracer actually may have contained some amount of ¹⁵NO₃⁻ to begin with.

Added to the text.

Incubations with low ambient [NO₃⁻] had high to δ(¹⁵N) values (>1000 ‰; Fig. S2). This is likely because NO₃⁻ is produced when sulfamic acid is added to NO₂⁻ (Granger and Sigman, 2009), so the sulfamic treatment probably chemically converted some ¹⁵N–NO₂⁻ tracer to ¹⁵N–NO₃⁻; additionally, ¹⁵N–NO₃⁻ is a possible contaminant of the ¹⁵N–NO₂⁻ tracer solutions.

L253: seawater water?

Corrected.

Reference materials were diluted from 200 mM working stocks into 3 mL NO₂⁻-free seawater in 5 and 10 nmol quantities of NO₂⁻ to correct for the contribution of a consistent blank to a range of sample sizes.

L256: ...precision for the denitrifier and azide methods is typically better...

Corrected.

The δ(¹⁵N) analytical precision for the denitrifier and azide methods is typically better (Sigman et al., 2001; McIlvin and Altabet, 2005), but tracer measurements tend to have lower analytical precision than natural abundance measurements.

L336: here the word ‘exchange’ is used to refer to movement of ¹⁵N from one pool to another occurring through biologically mediated processes. I would suggest using the word ‘transfer’ and not ‘exchange’ – as exchange is often used to refer to abiotic (or enzyme mediated) equilibration between two distinct pools.

Corrected here and throughout the text.

Rates of ¹⁵N and ¹⁴N transfer between substrate pools via NH₃ oxidation, NO₂⁻ oxidation, and NO₃⁻ reduction were also included in the model.

L348: extra comma

Corrected.

The model was optimized using the Nelder–Mead Simplex algorithm (Nelder and Mead, 1965), implemented in the Scipy optimization library (Virtanen et al., 2020), which has been used successfully for natural abundance N₂O isotopocule models (Monreal et al., 2022).

L395: With respect to the apparent negative nitrite oxidation rate – can any explanation here be invoked? Is this a real phenomenon or just some random analytical artifact that can't be easily explained?

The “negative” nitrite oxidation rates at two depths are likely an artifact of the elevated to $\delta^{15}\text{N}$ values in some of our $^{15}\text{N}\text{-NO}_2^-$ treatments (discussed above). We have added this to the text.

In some cases, NO_2^- oxidation rates appeared negative due to a decrease in $^{15}\text{N}\text{-NO}_3^-$ vs. incubation time (Fig. 3b, h), which was likely an artifact of the elevated to $\delta^{15}\text{N}$ values in some of our $^{15}\text{N}\text{-NO}_2^-$ treatments (discussed above).

L456: sediment-water interface?

This measurement was made at 898 m, which was very close to the bottom depth at station PS3. Clarified in the text.

At station PS3, there was also a small, significant rate of NH_3 oxidation (0.303 ± 0.005 nM N/day) at 898 m, which was close to the bottom depth (Fig. 3i).

L490: N_2O production pathways

Corrected.

The oxygen dependencies of N_2O production pathways were determined by fitting model derived N_2O production pathways vs. $[\text{O}_2]$ using the following rate law:

L725: depends on the ^{15}N content of each substrate

The conclusions have been modified to reflect the fact that we actually see approximately equal placement of NO_2^- -derived N and NH_4^+ -derived N in N^α and N^β , and thus that hybrid site preference may actually be constant (see response to L610 above).

Community Comment, Julie Granger

The authors present a supremely well executed study of N cycling rates in an oxygen deficient zones from well-controlled tracer incubations, from which they derive the relative contribution of respective processes to N₂O production, and from which they document the sensitivity of said production pathways to dissolved oxygen concentrations. Their tracer incubations rely in part on site-preference measurements of isotopocules in order to determine pathways of production. Their data corroborate a dominance of denitrification in N₂O production within the anaerobic regions of the water column, whereas multiple pathways operate concurrently in oxyclines. N₂O production from ammonium, presumed to be catalyzed by nitrifiers, occurred dominantly through a hybrid pathway reliant on both ammonium and nitrite as substrates, whereas the hydroxylamine pathway (both N's in N₂O from ammonium) was relegated to the well-oxygenated upper water column. The results and interpretation are highly informative, providing important constraints on pathways of N₂O production and their respective sensitivity to oxygen.

I found the manuscript generally well written but, perhaps necessarily, a challenging read. I read it multiple times. The “cognitive challenge” arises from the inherent complexity of the topic and study design. It is also exacerbated by some structural elements of the manuscript that would benefit from revision: (a) The motivations for the study are not made clear in the introduction; (b) the general “order of operation” keeps jumping around in the results and discussion (I explain what I mean below), (c) there is a heavy reliance on supplementary materials, requiring a lot of back and forth.

I suggest a number of modifications that I think could improve ease of understanding by readers peripheral to the field of N₂O isotopes who want to understand the findings and who also want to have a sense of the limitations of the findings.

Thank you for taking the time to thoroughly read and understand our paper, and for your constructive feedback. We have restructured the paper according to your suggestions and hope that it is easier to follow as a result.

The introduction does not effectively motivate the study. This study appears to be a companion to a published study where net rates of N cycling were determined from bulk tracer additions. I suppose that is why the bulk rate estimates figures were relegated to the supplements even though they are highly informative in the current context. Regardless, questions evidently emerged from the previous study that are presumably addressed herein, but these questions are not articulated in the introduction. I suggest the following paragraph sequence, which would make the intro more seamless:

The first paragraph alerts us that the study deals with nitrous oxide in oxygen deficient zones, with a justification of why N₂O matters. In the second paragraph, the reader expects to learn where N₂O is believed to come from in ODZ's. Instead, the paragraph otherwise begins with what seems a separate (but related) topic, N₂O production by archaea, ocean-wide, not necessarily in ODZ's. In lieu, I suggest moving up the third paragraph to the second, to explain the current understanding that most N₂O in ODZ's appears produced by denitrification. This would lead into a third paragraph that explains that nonetheless, a significant fraction appears to

be produced by archaeal nitrification. I would present the current evidence that supports this hypothesis, in order to motivate “looking” for hybrid production, which is where this paper ultimately brings us.

Thank you for this helpful suggestion. We moved up paragraph three of the introduction (N₂O production via denitrification) and revised (formerly) paragraph two to focus more on motivating our discussion of hybrid production.

Nitrous oxide (N₂O) is one of the lesser-known greenhouse gases, yet its potential to warm the environment, on a per-molecule basis, is immense. N₂O has a global warming potential 273 times that of carbon dioxide (Smith et al., 2021), and its atmospheric mixing ratio is increasing at a rate of 0.85±0.03 ppb/year (Tian et al., 2020). In the ocean, hotspots of N₂O production and flux to the atmosphere occur in marine oxygen deficient zones (ODZs), where steep redox gradients allow for multiple, overlapping N₂O production processes to occur (Codispoti and Christensen, 1985). ODZs have expanded over the last 60 years (Stramma et al., 2008; Breitburg et al., 2018) and will likely continue to do so as the oceans warm (Oschlies et al., 2018), although fate of the anoxic cores of ODZs ([O₂] ≤ 20 μmol/kg) remains uncertain (Cabré et al., 2015; Bianchi et al., 2018; Busecke et al., 2022). Without a clear picture of N₂O cycling in these regions, it is impossible to predict how climate change will impact the emission of this powerful greenhouse gas from the ocean.

Much of the N₂O cycling in ODZs is linked to denitrification. In low-oxygen waters, denitrifying organisms produce N₂O as an intermediate during organic matter remineralization (Zumft, 1997; Naqvi et al., 2000; Dalsgaard et al., 2014). Both direct rate measurements (Ji et al., 2015, 2018; Frey et al., 2020) and natural abundance isotope measurements (Kelly et al., 2021; Casciotti et al., 2018; Monreal et al., 2022; Toyoda et al., 2023) indicate that N₂O production directly from nitrate (NO₃⁻), i.e., without exchange with extracellular NO₂⁻ or NO pools, is the primary source of N₂O in ODZs. N₂O production from extracellular NO₂⁻, meanwhile, tends to occur at lower rates (Ji et al., 2015, 2018; Frey et al., 2020). Historically, N₂O production from denitrification was thought to cease at dissolved oxygen concentrations above 2–3 μM (Dalsgaard et al., 2014), but more recent data suggest that N₂O production from NO₃⁻ can occur at ambient oxygen levels as high as 30 μM (Ji et al., 2018; Frey et al., 2020). N₂O consumption via denitrification is more sensitive to oxygen than N₂O production via denitrification, leading to an oxygen window in which denitrification is a source but not a sink of N₂O (Babbín et al., 2015; Frey et al., 2020; Dalsgaard et al., 2014; Farías et al., 2009), although the oxygen inhibition constant for N₂O consumption remains difficult to define (Sun et al., 2021). N₂O may also be consumed through N₂O fixation, although the importance of N₂O fixation in the ocean has yet to be determined (Farías et al., 2013; Si et al., 2023).

Nonetheless, a significant fraction of the N₂O in the oxyclines above and below ODZs may be derived from archaeal nitrification. When nitrite (NO₂⁻) is present, isotopic evidence continues to suggest that ammonia-oxidizing archaea can produce N₂O via a hybrid mechanism that combines nitrogen (N) derived from nitrite (NO₂⁻) and ammonium (NH₄⁺) to form the N₂O molecule (Stieglmeier et al., 2014; Trimmer et al., 2016; Frame et al., 2017; Frey et al., 2020, 2023). New evidence indicates that ammonia-oxidizing archaea can produce N₂O both as a by-product of hydroxylamine oxidation and via hybrid N₂O production, and that the ratio of these processes depends on the ratio of NH₄⁺ to NO₂⁻ available to the archaea (Wan et al., 2023b).

The exact mechanism and enzymology of archaeal N₂O production remains unknown (Carini et al., 2018; Stein, 2019), but may involve a reaction between hydroxylamine and nitric oxide (NO), which occur as intermediates during archaeal ammonia oxidation (Vajrala et al., 2013; Martens-Habbenha et al., 2015; Kozłowski et al., 2016; Lancaster et al., 2018). In anaerobic conditions, ammonia-oxidizing archaea are also capable of NO dismutation to O₂ and N₂, which may involve N₂O as an intermediate (Kraft et al., 2022). Ammonia-oxidizing bacteria, more common in regions that are nutrient replete, produce N₂O as a byproduct of hydroxylamine oxidation (Cohen and Gordon, 1979), and via nitrifier-denitrification as oxygen concentrations decline (Goreau et al., 1980; Wrage et al., 2001; Stein and Yung, 2003) and nitrite concentrations rise (Frame and Casciotti, 2010).

The fourth paragraph should be explicit in whether it is referring to naturally occurring isotopes or tracer isotopes, since the subsequent paragraph jumps into tracers. To better motivate the study, perhaps this section can explain what naturally occurring isotopocules have divulged about N₂O production in ODZ's specifically, and which questions remain unanswered – in order to link to the last paragraph of the intro.

We made it more explicit that paragraph four is about natural abundance isotopes. We also revised it to focus on the fact that hybrid N₂O production complicates the interpretation of natural abundance $\delta(^{15}\text{N}^{\text{sp}})$ because it draws from two different substrate pools.

The stable, natural abundance nitrogen and oxygen isotopes of N₂O can provide quantification of – and distinction among – potential N₂O cycling mechanisms (Kim and Craig, 1990; Rahn and Wahlen, 2000; Toyoda and Yoshida, 1999). For example, natural abundance N₂O isotopocule studies have indicated that the high, near-surface N₂O accumulations in the eastern tropical North Pacific (ETNP) ODZ are 80% derived from denitrification and 20% derived from nitrification (Kelly et al., 2021). The isotopic content of the individual nitrogen and oxygen atoms in the N₂O molecule are expressed in delta notation, defined as $\delta(^{15}\text{N})$ or $\delta(^{18}\text{O}) = (R_{\text{sample}}/R_{\text{standard}} - 1)$, where R_{standard} for $\delta(^{15}\text{N})$ and $\delta(^{18}\text{O})$ are the ratios $^{15}\text{N}/^{14}\text{N}$ of air and $^{18}\text{O}/^{16}\text{O}$ of Vienna Standard Mean Ocean Water (VSMOW), respectively (Kim and Craig, 1990; Rahn and Wahlen, 2000; Toyoda and Yoshida, 1999). In addition to the bulk nitrogen and oxygen isotope ratios in N₂O, we can measure the isotopic content of the inner (α) nitrogen atom and an outer (β) nitrogen atom in N₂O (Toyoda and Yoshida, 1999; Brenninkmeijer and Röckmann, 1999). The difference in the ^{15}N content of these two atoms is often referred to as the 'site preference' and is defined as $\delta(^{15}\text{N}^{\text{sp}}) = \delta(^{15}\text{N}^{\alpha}) - \delta(^{15}\text{N}^{\beta})$. In natural abundance studies, $\delta(^{15}\text{N}^{\text{sp}})$ is particularly useful because it exhibits distinct values for different N₂O production processes, independent of the isotopic value of the substrate (Toyoda et al., 2002; Sutka et al., 2003, 2006, 2004; Toyoda et al., 2005; Frame and Casciotti, 2010). This allows for partitioning between different N₂O sources, and has been used extensively to quantify N₂O cycling in the ocean (Toyoda et al., 2002, 2019, 2021, 2023; Popp et al., 2002; Toyoda et al., 2005; Yamagishi et al., 2007; Westley et al., 2006; Fariás et al., 2009; Bourbonnais et al., 2017, 2023; Casciotti et al., 2018; Kelly et al., 2021; Monreal et al., 2022). As we elaborate upon in the discussion, however, the premise that $\delta(^{15}\text{N}^{\text{sp}})$ exhibits a unique and consistent value depends on the assumption that both N atoms in N₂O are derived from a singular substrate pool. Thus, hybrid N₂O production may complicate traditional interpretations of natural abundance N₂O isotopocules.

IN the last paragraph, the motivation for measuring site preference on tracer experiments needs clearer articulation. What additional insights can it provide that natural abundance or bulk tracer experiments did not? And your results, as I see them, inform on more than a dependence of oxygen on hybrid production, correct? They (a) corroborate previous findings on relative pathways of N₂O production (b) uncover that the hybrid pathway dominates production by nitrification and (c) production from hydroxylamine is not a thing except at the surface. Importantly, do the results confirm inferences from natural abundance tracers in the same system? These can be posed as questions to which the authors can return in the discussion.

We added a sentence to the last paragraph saying that $^{45}\text{N}_2\text{O}^\alpha$ and $^{45}\text{N}_2\text{O}^\beta$ measurements create an additional constraint on N₂O production rates and thus allow us to quantify different source process more precisely and accurately. As per your suggestion, we also detailed more thoroughly the different findings from this study.

Previous studies have used ^{15}N tracer experiments to measure N₂O production rates in ODZs (Ji et al., 2015, 2018; Frey et al., 2020, 2023). These studies used the accumulation of $^{45}\text{N}_2\text{O}$ and $^{46}\text{N}_2\text{O}$ resulting from the addition of ^{15}N -labeled substrates such as $^{15}\text{NH}_4^+$ and $^{15}\text{NO}_2^-$ to measure N₂O production rates. To our knowledge, however, the isotopomer measurement has never been applied to ^{15}N -tracer experiments to track ^{15}N from different substrates into the α and β positions of the N₂O molecule. Here, we present data showing the production of N₂O isotopomers with ^{15}N in the α position ($^{45}\text{N}_2\text{O}^\alpha$) and ^{15}N in the β position ($^{45}\text{N}_2\text{O}^\beta$) from ^{15}N -labeled NH_4^+ , NO_2^- , and NO_3^- . Measuring the production of $^{45}\text{N}_2\text{O}^\alpha$ and $^{45}\text{N}_2\text{O}^\beta$ creates an additional constraint on N₂O production mechanisms and thus allows us to quantify different source process more precisely and accurately. We employed these measurements to (a) validate previous ^{15}N tracer studies of N₂O production rates in the ETNP, (b) uncover that the hybrid pathway dominates production by nitrification, (c) establish the insignificance of production from solely NH_4^+ except the surface, and (d) infer a constant $\delta(^{15}\text{N}^{\text{sp}})$ for hybrid N₂O, despite drawing from two substrate pools. We also use these results to confirm inferences from natural abundance N₂O isotopocules measured in the same system (Kelly et al., 2021).

Methods:

Line 200: I would rephrase to “... contribution of $^{15}\text{N}^{15}\text{NO}$ to masses 46 and 31, which, while negligible at natural abundance, becomes important in tracer experiments.”

Corrected.

The number ratios of isotopomers $^{14}\text{N}^{15}\text{NO}$ and $^{15}\text{N}^{14}\text{NO}$ were calculated as in Kelly et al., 2023, with the following modifications to account for contribution of $^{15}\text{N}^{15}\text{NO}$ to the molecular ion number ratios 46/44 (^{46}R) and 31/30 (^{31}R), which, while negligible at natural abundance, becomes important in tracer experiments.

Equations 1-4: I think it would be wise to define ALL the terms in equations 1-4, for readers peripheral to this field who may still strive to understand the equations.

Corrected.

In natural abundance samples, pyisotopomer solves the following four equations to obtain $^{15}\text{R}^\alpha$ and $^{15}\text{R}^\beta$:

$$^{45}\text{R} = ^{15}\text{R}^\alpha + ^{15}\text{R}^\beta + ^{17}\text{R} \quad (1)$$

$$^{46}\text{R} = (^{15}\text{R}^\alpha + ^{15}\text{R}^\beta)^{17}\text{R} + ^{18}\text{R} + ^{15}\text{R}^\alpha ^{15}\text{R}^\beta \quad (2)$$

$$^{17}\text{R}/^{17}\text{R}_{\text{VSMOW}} = (^{18}\text{R}/^{18}\text{R}_{\text{VSMOW}})^\beta [\Delta(^{17}\text{O}) + 1] \quad (3)$$

$$^{31}\text{R} = \frac{(1 - \gamma)^{15}\text{R}^\alpha + \kappa^{15}\text{R}^\beta + ^{15}\text{R}^\alpha ^{15}\text{R}^\beta + ^{17}\text{R}[1 + \gamma^{15}\text{R}^\alpha + (1 - \kappa)^{15}\text{R}^\beta]}{1 + \gamma^{15}\text{R}^\alpha + (1 - \kappa)^{15}\text{R}^\beta} \quad (4)$$

Where ^{45}R , ^{46}R , and ^{31}R are the molecular ion number ratios 45/44, 46/44, and 31/30. $^{15}\text{R}^\alpha$, $^{15}\text{R}^\beta$, ^{17}R and ^{18}R denote the number ratios of $^{14}\text{N}^{15}\text{N}^{16}\text{O}$, $^{15}\text{N}^{14}\text{N}^{16}\text{O}$, $^{14}\text{N}_2^{17}\text{O}$, and $^{14}\text{N}_2^{18}\text{O}$, respectively, to $^{14}\text{N}_2^{16}\text{O}$. Here, $\Delta(^{17}\text{O})$ was assumed to be equal to 0. In these equations, the term $(^{15}\text{R}^\alpha)^{15}\text{R}^\beta$ represents the statistically expected contribution of $^{15}\text{N}^{15}\text{N}^{16}\text{O}$ to the ^{46}R and ^{31}R ion number ratios, based on the probabilities of forming $^{15}\text{N}^{15}\text{N}^{16}\text{O}$. The probability of getting ^{15}N in N^α is given by $^{15}\text{R}^\alpha$ and the probability of getting ^{15}N in N^β is given by $^{15}\text{R}^\beta$; furthermore, the two probabilities are assumed to be independent, so the probability of getting ^{15}N in both positions would be $(^{15}\text{R}^\alpha)^{15}\text{R}^\beta$ (Kaiser et al., 2004). Predicting the concentration of $^{15}\text{N}^{15}\text{N}^{16}\text{O}$ from the distribution of ^{15}N in the singly-labeled molecules ($^{15}\text{R}^\alpha$ and $^{15}\text{R}^\beta$) is a reasonable assumption for natural abundance samples, where the concentration of $^{15}\text{N}^{15}\text{N}^{16}\text{O}$ is extremely low (Magyar et al., 2016; Kantnerová et al., 2022).

Line 245: Nitrate IS produced from nitrite when sulfamic acid (or any acid) is added to nitrite, due to the acid decomposition of nitrous acid. See Granger and Sigman 2009, Equations 6 and Figure 2. And ^{15}N nitrate is a probable contaminant of the ^{15}N nitrite solutions.

We revised this section to say that our high $\delta^{15}\text{N}$'s are likely because NO_3^- is produced when sulfamic acid is added to NO_2^- (Granger and Sigman, 2009), so the sulfamic treatment probably chemically converted some $^{15}\text{N}\text{-NO}_2^-$ tracer to $^{15}\text{N}\text{-NO}_3^-$; additionally, $^{15}\text{N}\text{-NO}_3^-$ is a probable contaminant of the $^{15}\text{N}\text{-NO}_2^-$ tracer solutions.

Incubations with low ambient $[\text{NO}_3^-]$ had high to $\delta(^{15}\text{N})$ values (>1000 ‰; Fig. S2). This is likely because NO_3^- is produced when sulfamic acid is added to NO_2^- (Granger and Sigman, 2009), so the sulfamic treatment probably chemically converted some $^{15}\text{N}\text{-NO}_2^-$ tracer to $^{15}\text{N}\text{-NO}_3^-$; additionally, $^{15}\text{N}\text{-NO}_3^-$ is a possible contaminant of the $^{15}\text{N}\text{-NO}_2^-$ tracer solutions. Regardless, this would have shifted all three timepoints equally, and thus should not introduce a bias into the slope of $\delta(^{15}\text{N}\text{-NO}_3^-)$ with time and the rates calculated there from.

Line 274: what is N exchange between substrates?

Sorry, “exchange” is probably the wrong word here. We have changed it to N transfer between substrates.

While it is possible to calculate rates of hybrid and bacterial N_2O production with linear regressions of $^{45}\text{N}_2\text{O}$ and $^{46}\text{N}_2\text{O}$ with time (Trimmer et al., 2016), these calculations cannot take into account ^{15}N transfer between substrates, and more importantly, produce separate rate estimates for separate tracer experiments.

Line 280: These “pathways” were not discovered by Wan et al. 2023. The citations are unclear to me.

We changed these citations to “referred to as Pathway 1 in Wan et al., 2023...”.

The model encoded four different N₂O producing pathways: 1) **production from solely NH₄⁺**, which includes N₂O from hydroxylamine oxidation (referred to as Pathway 1 in Wan et al., 2023), hybrid production using cellular NO₂⁻ (referred to as Pathway 2 in Wan et al., 2023) and nitrifier–denitrification using cellular NO₂⁻; 2) **hybrid production** using extracellular NO₂⁻ (referred to as Pathway 3 in Wan et al., 2023); 3) **production from NO₂⁻**, i.e. denitrification or nitrifier–denitrification using extracellular NO₂⁻; and 4) **production from NO₃⁻**, i.e. denitrification using cellular NO₂⁻ (Fig. 2).

Results:

I realize some of the data are published elsewhere but they are fundamental to navigating the paper. I suggest moving some of these back to the main text. In particular, the N₂O production plots (mass 45 for each 15N substrate).

To clarify: none of the data included in this study have been published elsewhere. A companion paper (Frey et al., 2023) published rates of ammonia oxidation and N₂O production from ammonium measured in concurrent, but separate, experiments. Nevertheless, we have moved the ⁴⁵N₂O and ⁴⁶N₂O production plots into the main text. They are now figures 4 and 5.

I suggest presenting the results in order of dominance of rates, and sticking to this pattern in all subsequent text and figures. Denitrification is fastest; detailing it first helps contextualize nitrite oxidation rates, which are also very high, and ammonium oxidation rates, which are puny.

We changed the order of section 3.2, “Nitrification and nitrate reduction rates,” to talk about denitrification first, then nitrite oxidation, then ammonia oxidation.

3.2 Nitrification and nitrate reduction rates

NO₃⁻ reduction to NO₂⁻ occurred at rates ranging from 0.54±0.04 to 33.2±0.1 nM N/day (Table S2). There was a small, significant rate of NO₃⁻ reduction to NO₂⁻ in apparently aerobic waters near the surface at station PS1 (Fig. 3a). The highest rates of NO₃⁻ reduction to NO₂⁻ occurred in the deep, anoxic waters at station PS2 (33.24±0.01 nM N/day; Fig. 3d) and in the secondary chlorophyll maximum at station PS3 (19.2±0.1 nM N/day; Fig. 3g).

NO₂⁻ oxidation rates ranged from 13.05±0.08 nM N/day to 465±86 nM N/day (Table S2). The highest rates of NO₂⁻ oxidation occurred within apparently oxygen deficient waters, at 81.0±0.2 nM N/day in the secondary chlorophyll a maximum at station PS2 and at 465±86 nM N/day in the secondary NO₂⁻ maximum at station PS3 (Fig. 3e, h; Table S2). Note that these are potential rates, since the ¹⁵N addition was generally much greater than the ambient concentration (Lipschultz, 2008). In some cases, NO₂⁻ oxidation rates appeared negative due to a decrease in ¹⁵N–NO₃⁻ vs. incubation time (Fig. 3b, h), which was likely an artifact of the elevated to δ(¹⁵N) values in some of our ¹⁵N–NO₂⁻ treatments (discussed above). We chose, however, not to left censor the data.

NH₃ oxidation to NO₂⁻ occurred at small, but significant rates ranging from 0.19±0.0004 nM N/day to 4.68±0.07 nM N/day (Table S2). At every station, rates of NH₃ oxidation peaked near the base of the mixed layer, at the same depth as the near–surface [N₂O] maximum (Fig. 3c, f, i). At station PS2, NH₃ oxidation showed a secondary peak at the same depth as the deep [N₂O]

maximum (Fig. 3f). At station PS3, there was also a small, significant rate of NH_3 oxidation (0.303 ± 0.005 nM N/day) at 898 m, which was close to the bottom depth (Fig. 3i). Rates of NH_3 oxidation were generally lower than NO_2^- oxidation and undetectable in oxygen deficient waters (Fig. 3c, f, i).

Stick with one, NH_3 or NH_4 oxidation. It varies in the text.

We changed all of these to NH_3 oxidation.

Section 3.3 is very difficult to navigate. I read it multiple times. The term “high rates” is meaningless without context. Rates peak or not, but it can’t be argued that rates of $^{45}\text{N}_2\text{O}$ -alpha are high even in this context, at picomolar per day. In this regard, I suggest using picomolar in lieu of multiple decimals in the text and figures, which are tiresome. And the Figure S8 is nearly impossible to navigate as every panel has a different x axis range. Perhaps homogenize ranges for given isotopocule production? And I’m not sure why these figures are relegated to the supplements. I spent a long time looking at them. A long time...

You’re right, in this section “high rates” is relative. We revised “high rates” to “relatively higher rates.”

At each station, the observed rates of net $^{46}\text{N}_2\text{O}$ (Fig. 4), $^{45}\text{N}_2\text{O}^\alpha$ and $^{45}\text{N}_2\text{O}^\beta$ (Fig. 5) production from $^{15}\text{N}-\text{NH}_4^+$, $^{15}\text{N}-\text{NO}_2^-$, and $^{15}\text{N}-\text{NO}_3^-$ all peaked at or just below the oxic–anoxic interface, where the near surface $[\text{N}_2\text{O}]$ maximum was found. There were also relatively higher rates of net $^{46}\text{N}_2\text{O}$ production from $^{15}\text{N}-\text{NO}_2^-$ and $^{15}\text{N}-\text{NO}_3^-$ within the secondary NO_2^- maximum (253 m) at station PS2 (Fig. 4d–e). Relatively high rates of net $^{45}\text{N}_2\text{O}^\alpha$ and $^{45}\text{N}_2\text{O}^\beta$ production also occurred in the secondary NO_2^- maximum at stations PS2 (253m; Fig. 5d–e) and PS3 (182 m; Fig. 5g–h). The net rates of $^{45}\text{N}_2\text{O}^\alpha$ and $^{45}\text{N}_2\text{O}^\beta$ production varied in concert at almost every station and depth, with a few exceptions (Fig. 5).

We changed all of the N_2O production rates from nM/day to pM/day, here and throughout the text.

For example, in the secondary NO_2^- maximum (182 m) at station PS3, in the $^{15}\text{N}-\text{NO}_2^-$ experiment, the production of $^{45}\text{N}_2\text{O}^\alpha$ was 60 ± 30 pM $\text{N}_2\text{O}/\text{day}$ ($p = 0.09$) and there was no significant production of $^{45}\text{N}_2\text{O}^\beta$ (Fig. 5h). In the parallel $^{15}\text{N}-\text{NH}_4^+$ experiment, the production of $^{45}\text{N}_2\text{O}^\beta$ was 0.7 ± 0.3 pM $\text{N}_2\text{O}/\text{day}$ ($p = 0.06$) and there was no significant production of $^{45}\text{N}_2\text{O}^\alpha$. At this station and depth, f (the proportion of N^α derived from NO_2^-) was equal to 0.9 ± 0.2 (Table S4). The second experiment in which labeling was unequal occurred at the oxic–anoxic interface (92 m) at station PS2, where in the $^{15}\text{N}-\text{NH}_4^+$ experiment, the production of $^{45}\text{N}_2\text{O}^\alpha$ was 5 ± 2 pM $\text{N}_2\text{O}/\text{day}$ ($p = 0.02$) and there was no significant production of $^{45}\text{N}_2\text{O}^\beta$ (Fig. 5f). Here, f was equal to 0.2 ± 0.1 . Finally, at the mid–oxycline depth (25 m) at station PS3, in the $^{15}\text{N}-\text{NH}_4^+$ experiment, the production of $^{45}\text{N}_2\text{O}^\alpha$ was 0.23 ± 0.8 pM $\text{N}_2\text{O}/\text{day}$ ($p = 0.02$) and there was no significant production of $^{45}\text{N}_2\text{O}^\beta$. Here, f was statistically indistinguishable from 0.

We homogenized the x-axis ranges for Fig. S7 and Fig. S8 as much as possible while still allowing the variation in each panel to be visualized and moved Fig. S7 and Fig. S8 to the main text. They are now Figs. 4 and 5.

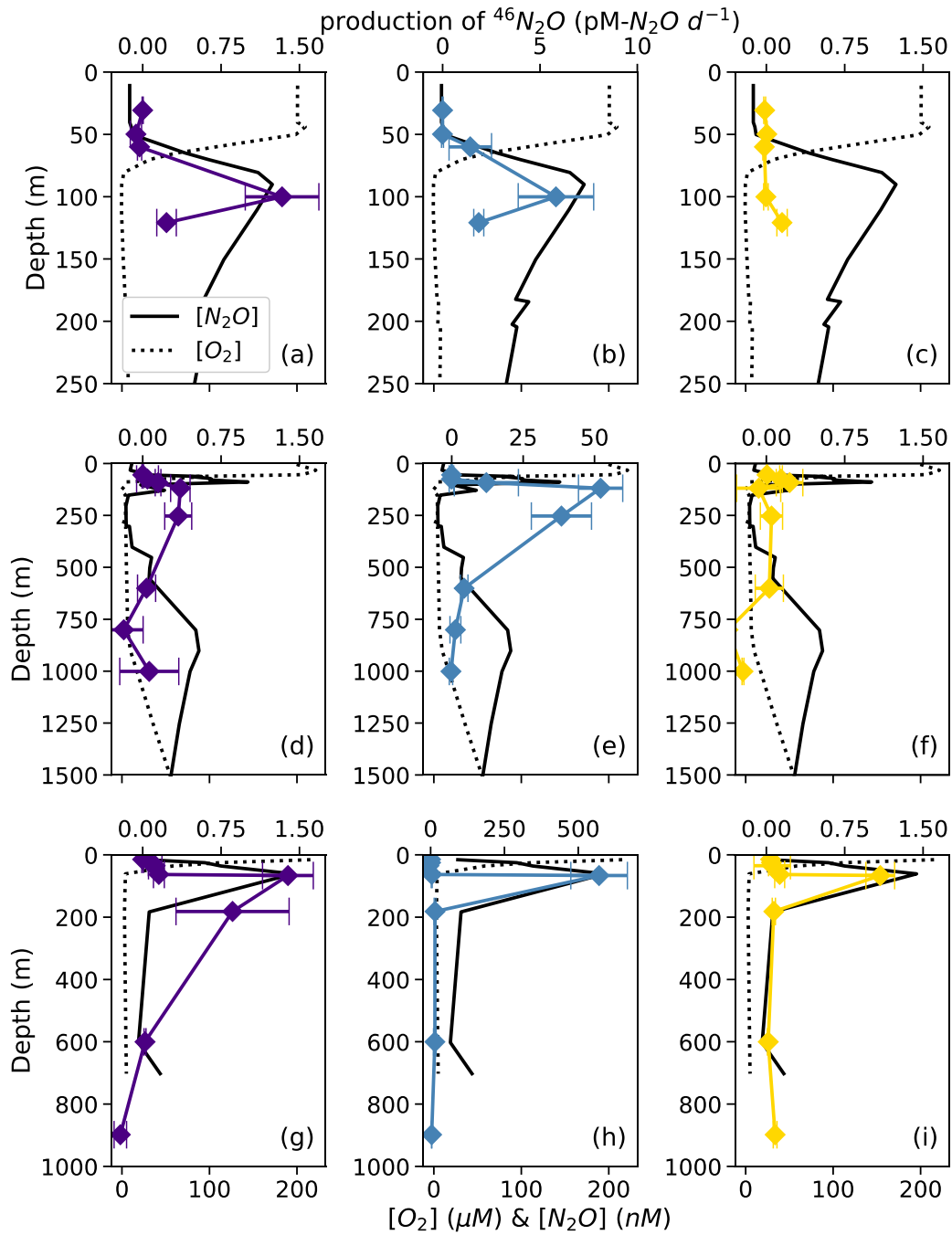


Figure 4. Net $^{46}\text{N}_2\text{O}$ production from $^{15}\text{N}\text{-NO}_3^-$ (a, d, g, indigo), $^{15}\text{N}\text{-NO}_2^-$ (b, e, h, blue), and $^{15}\text{N}\text{-NH}_4^+$ (c, f, i, yellow) at stations PS1 (a-c), PS2 (d-f), and PS3 (g-i). N_2O production rates are plotted over depth profiles of dissolved $[\text{O}_2]$ (dashed lines) and $[\text{N}_2\text{O}]$ (solid lines, from Kelly et al., 2021). Error bars are calculated from linear regression slope error of $^{46}\text{N}_2\text{O}$ vs. incubation time. Note the different x-axis scales for $^{46}\text{N}_2\text{O}$ production (top) and $[\text{O}_2]$ and $[\text{N}_2\text{O}]$ (bottom).

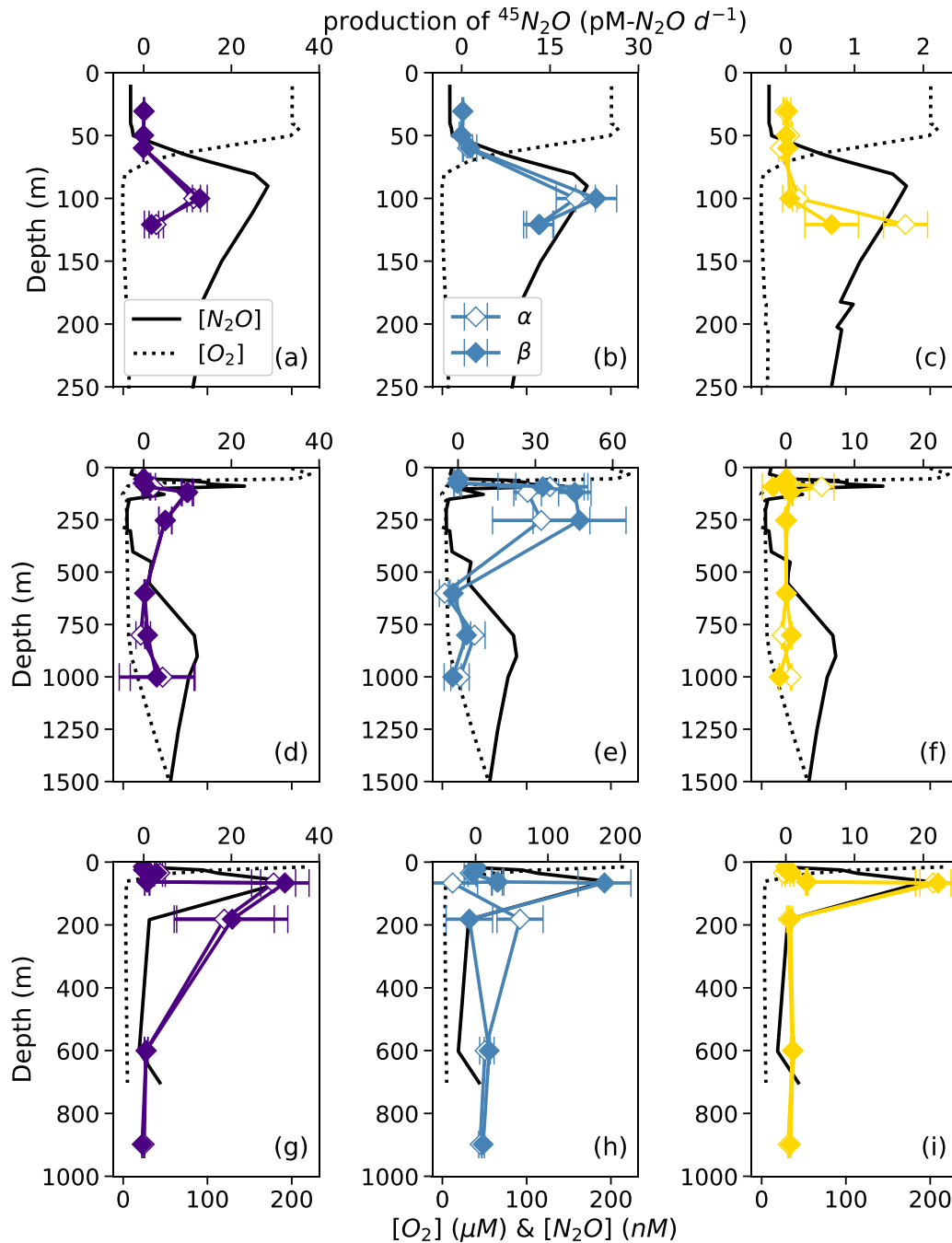


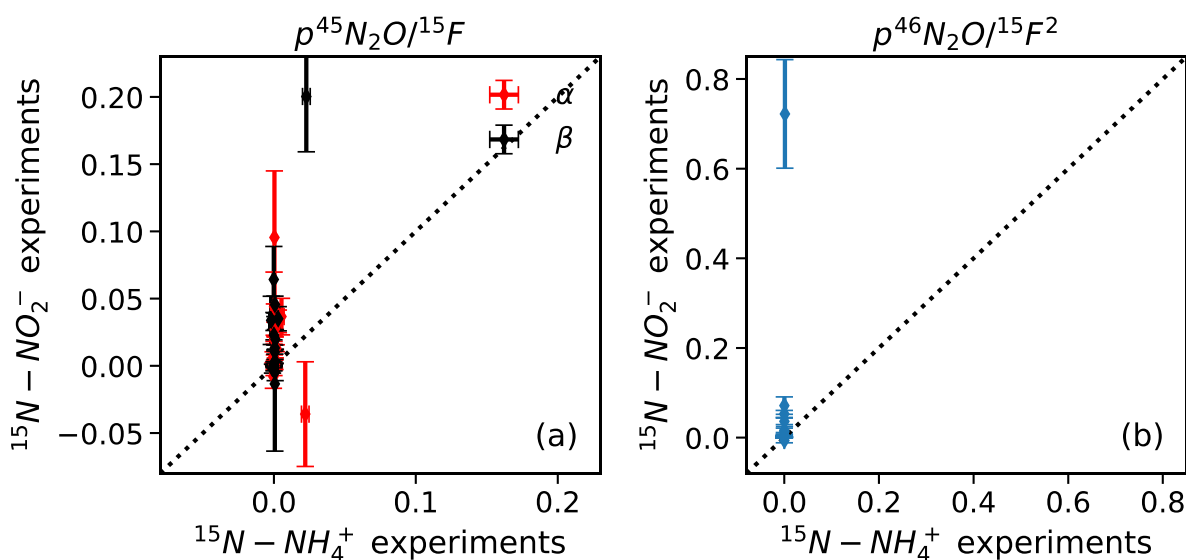
Figure 5. Net $^{45}\text{N}_2\text{O}^\alpha$ (open symbols) and $^{45}\text{N}_2\text{O}^\beta$ (closed symbols) production from $^{15}\text{N-NO}_3^-$ (a, d, g, indigo), $^{15}\text{N-NO}_2^-$ (b, e, h, blue), and $^{15}\text{N-NH}_4^+$ (c, f, i, yellow) at stations PS1 (a–c), PS2 (d–f), and PS3 (g–i). N_2O production rates are plotted over depth profiles of dissolved $[\text{O}_2]$ (dashed lines) and $[\text{N}_2\text{O}]$ (solid lines, from Kelly et al., 2021). Error bars are calculated from linear regression slope error of $^{45}\text{N}_2\text{O}$ vs. incubation time. Note the different x-axis scales for $^{45}\text{N}_2\text{O}$ production (top) and $[\text{O}_2]$ and $[\text{N}_2\text{O}]$ (bottom).

The line at 215 belongs with the previous paragraph. And it's not clear whether this will be an example of rates varying in concert or not. Wordsmith accordingly.

Did you mean a different line? 215 is just after eqn. (6), “where $^{15}\text{N}^{15}\text{N}^{16}\text{O}_{\text{excess}}$ represents the amount of $^{15}\text{N}^{15}\text{N}^{16}\text{O}$ produced in the sample over the course of the experiment.”

Equation 13: In the case of nitrite where a higher concentration was added than intended, I would think that the flux derived therefrom, J , is no longer proportional to nitrite (zero order) at these concentrations. Does this matter?

If we compare the ^{15}N -labeled ammonium treatment to the ^{15}N -labeled nitrite treatment at the same experimental depth, the $^{45}\text{N}_2\text{O}$ and $^{46}\text{N}_2\text{O}$ production rates in the ^{15}N -labeled nitrite treatment were far higher than those in the ^{15}N -labeled ammonium treatment, even when normalized by atom fraction. This is visualized below. In fact, the rates of production of $^{45}\text{N}_2\text{O}$ and $^{46}\text{N}_2\text{O}$ in the ^{15}N -labeled ammonium treatments were so small, comparatively, that they are visually indistinguishable from zero when plotted on the same scale as the rates of production of $^{45}\text{N}_2\text{O}$ and $^{46}\text{N}_2\text{O}$ in the ^{15}N -labeled nitrite treatments.



Production of $^{45}\text{N}_2\text{O}$, divided by atom fraction, in the ^{15}N - NO_2^- treatment vs. ^{15}N - NH_4^+ treatment at the same experimental depths. Red diamonds indicate $p^{45}\text{N}_2\text{O}^\alpha/^{15}\text{F}$ and black diamonds indicate $p^{45}\text{N}_2\text{O}^\beta/^{15}\text{F}$. b) Production of $^{46}\text{N}_2\text{O}$, divided by atom fraction squared, in the ^{15}N - NO_2^- treatment vs. ^{15}N - NH_4^+ treatment at the same experimental depths. In both plots, the dashed line is the 1:1 line.

Since the tracer concentration was much higher in the ^{15}N -labeled nitrite treatment (5.00 μM) than in the ^{15}N -labeled ammonium treatment (0.501 μM), this imbalance of $^{45}\text{N}_2\text{O}$ production supports the idea that there is some dependence of N_2O production rate on substrate concentration.

Line 337: Wording of sentence is awkward.

Revised to:

The model solves for N_2O production rates, given a set of NH_3 oxidation, NO_2^- oxidation, and NO_3^- reduction rates calculated in Sect. 2.5, eqn. (7) (Table S2).

Line 395: How can nitrite oxidation rates possibly be negative?

The “negative” nitrite oxidation rates at two depths are likely an artifact of the elevated to $\delta(^{15}\text{N})$ values in some of our $^{15}\text{N}\text{-NO}_2^-$ treatments (discussed above). We have added this to the text.

In some cases, NO_2^- oxidation rates appeared negative due to a decrease in $^{15}\text{N}\text{-NO}_3^-$ vs. incubation time (Fig. 3b, h), which was likely an artifact of the elevated to $\delta(^{15}\text{N})$ values in some of our $^{15}\text{N}\text{-NO}_2^-$ treatments (discussed above).

Line 420: Remind the reader what “f” designates.

Done.

At this station and depth, f (the proportion of N^α derived from NO_2^-) was equal to 0.9 ± 0.2 (Table S4).

Equation 19: “AP” was designated as “15F” in equations above...

Changed to ^{15}F .

$$p_{\text{excess}}^{45} = p^{45} - p_{\text{expected}}^{45} = p^{45} - \frac{p^{46}}{^{15}\text{F}} 2(1 - ^{15}\text{F}) \quad (19)$$

Could $p_{45\text{excess}}$ result from misestimation of the actual atom percent of substrates the incubations? The rates are very small such having a small error on AP could potentially account for this? Or wrong proportion of carrier? I think Figure S9 may allude to this but the associated uncertainty needs to be better explained in the main text, whether or not the data evince unequal values of “f” beyond a reasonable “doubt”

Figure S9 (now Fig. S S7) alludes to this. The dashed lines in Figure S9 indicate the range of atom fractions in each type of experiment, which far exceeds the uncertainty in the atom fraction of any one individual experiment. So points above the dashed line indicate excess $^{45}\text{N}_2\text{O}$ production, beyond a reasonable doubt.

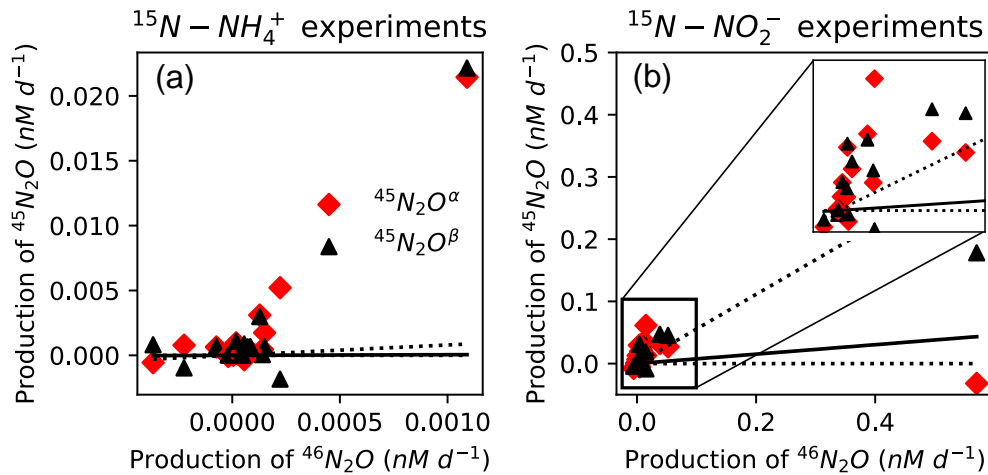


Figure S7. Net production of $^{45}\text{N}_2\text{O}^\alpha$ (red diamonds) and $^{45}\text{N}_2\text{O}^\beta$ (black triangles) vs. $^{46}\text{N}_2\text{O}$ from $^{15}\text{N}\text{-NH}_4^+$ (a) and $^{15}\text{N}\text{-NO}_2^-$ (b). The insert in (b) shows a zoomed-in view of the data. The solid black lines indicate the expected production $^{45}\text{N}_2\text{O}^\alpha$ and $^{45}\text{N}_2\text{O}^\beta$ from a process drawing both N atoms in N_2O from the same substrate pool, based on the atom fraction of the labeled substrate (NH_4^+ or NO_2^-) and a binomial distribution of N_2O isotopocules. Dashed lines indicate the range of expected values, based on the range of atom fractions in each experiment. Production of $^{45}\text{N}_2\text{O}^\alpha$ and $^{45}\text{N}_2\text{O}^\beta$ above this expected production indicate the presence of a hybrid process.

Figure 4: Present in order brought up in text, which is N₂O production from nitrate first. Is production from NH₄⁺ only necessarily hydroxylamine oxidation? It is called that in some figure captions. If so, it would be much easier for readers if it were called hydroxylamine oxidation throughout.

The order of this figure (now Figure 6) has been changed. Sorry, “hydroxylamine oxidation” was a mistake — N₂O from NH₄⁺ could also include hybrid production using an internal NO₂⁻ pool. We have revised the figure captions to “N₂O production from solely NH₄⁺”.

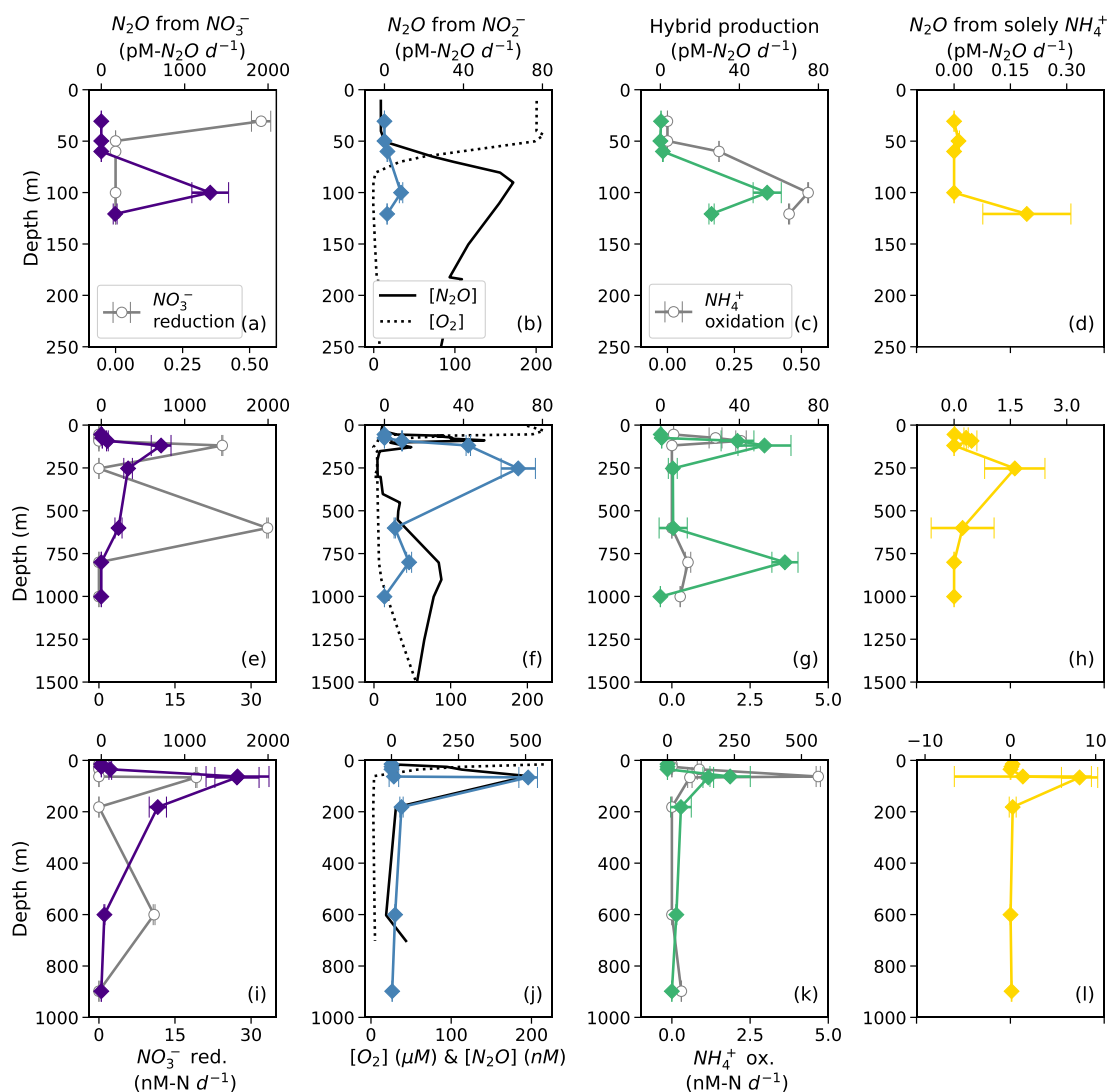


Figure 6. N₂O production from NO₃⁻ (a, e, i, indigo diamonds), N₂O production from NO₂⁻ (b, f, j, blue diamonds), hybrid N₂O production (c, g, k, green diamonds), and N₂O production from solely NH₄⁺ (d, h, l, yellow diamonds) at stations PS1 (a–d), PS2 (e–h), and PS3 (i–l). Panels a, e, and i also show rates of NO₃⁻ reduction to NO₂⁻ (open circles). Panels b, f, and j show depth profiles of dissolved [O₂] (dashed lines) and [N₂O] (solid lines, from Kelly et al., 2021). Panels c, g, and k show rates of NH₃ oxidation (gray circles). N₂O production rate error bars are calculated from 100 model optimizations, varying key parameters by up to 25%. Note the different x-axis scales for NO₃⁻ reduction to NO₂⁻ (a, e, i, bottom), N₂O production (top), [O₂] and [N₂O] (b, f, j, bottom), and NH₃ oxidation (c, g, k, bottom).

Section 3.5: I would start with describing N₂O production “as a whole”, followed by nitrate reduction (highest flux), etc... Same order of operation as suggested above.

We changed the order of section 3.5 to discuss N₂O production from nitrate first. We also changed the corresponding section of the discussion (Section 4.4).

3.5 Oxygen dependence of N₂O production

The oxygen dependencies of N₂O production pathways were determined by fitting model derived N₂O production pathways vs. [O₂] using the following rate law:

$$\text{rate} = ae^{-b[\text{O}_2]} \quad (21)$$

In this analysis, both ambient [O₂] measured by the Sea–Bird sensor mounted on the rosette (“ambient [O₂]”) and [O₂] measured by chemiluminescent optodes mounted inside incubation bottles (“incubation [O₂]”) were examined. The rate dependencies on ambient and incubation [O₂] reflect both preconditioning (i.e., the ambient [O₂] in which the microbial community was living before the incubation experiment), and response to perturbation (i.e., the experimental conditions inside the incubation bottles, if different from the environment). Those incubations that had higher incubation [O₂] than the ambient [O₂], had received small oxygen perturbations.

N₂O production via denitrification exhibited an exponentially declining relationship with dissolved O₂, where N₂O production from NO₂⁻ was more inhibited by dissolved O₂ than N₂O production from NO₃⁻ (Fig. 8). When looking at the oxygen dependence of denitrification, we found several instances of N₂O production from NO₃⁻ via denitrification with dissolved [O₂] greater than 3 μM (Fig. 8a–b). For example, at the oxic–anoxic interface at station PS2, where ambient [O₂] was 6.49 μM and incubation [O₂] was 6.29±0.07 μM (Table S1), N₂O production from NO₃⁻ was 70±10 pM N₂O/day (Fig. 6e, Table S4). N₂O production from NO₂⁻ at the same station and depth was 8.9±0.2 pM N₂O/day (Fig. 6f, Table S4). Similarly, at the oxic–anoxic interface of station PS3, where ambient [O₂] was 12.48 μM and incubation [O₂] was 6.64±0.03 μM (Table S1), N₂O production from NO₃⁻ was 120±20 pM N₂O/day (Fig. 6i, Table S4). There were also two anoxic depths at station PS2 that were not sparged with He before tracer addition (“base of ODZ” and “deep ODZ core”), where ambient [O₂] was below detection but incubation [O₂] was significantly elevated (17.7±0.1 μM and 19.2±0.8 μM, respectively; Table S1). At these depths, N₂O production from NO₂⁻ was 12±1 pM N₂O/day and 5.2±0.4 pM N₂O/day, respectively (Fig. 6f, Table S4). N₂O production from NO₃⁻ at the “deep ODZ core” depth was 210±40 pM N₂O/day (Table S4).

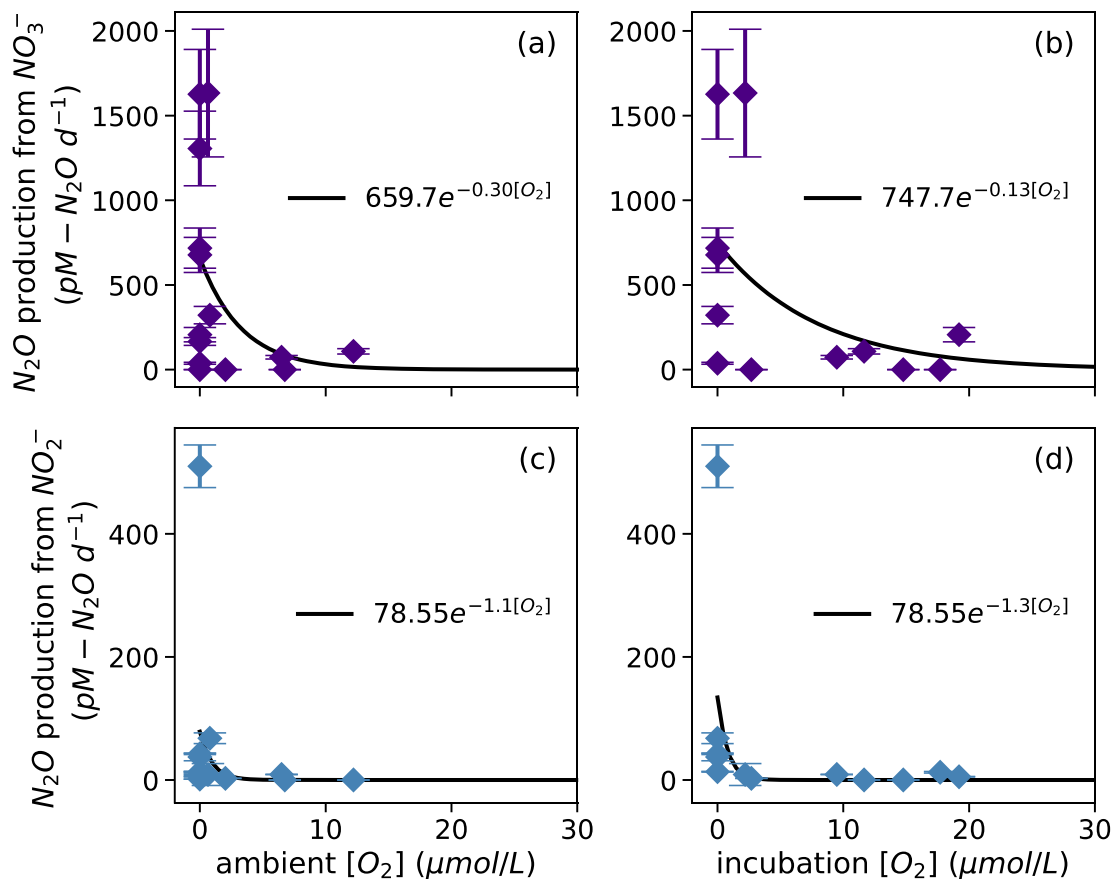


Figure 8. N_2O production from NO_3^- via denitrification (a, b) and from NO_2^- via denitrification (c, d), measured at a range of $[O_2]$ measured by a Seabird sensor (a, c) or by chemiluminescent optodes mounted inside incubation bottles (b, d). Curves of form $yield = ae^{-0.2b}$ are fit through the data (black lines); values of a and b are shown in white boxes in each plot.

Hybrid N_2O production rates also decreased exponentially with increasing dissolved $[O_2]$ (Fig. 9a–b). Fitting hybrid rates vs. ambient $[O_2]$ produced a rate equation (21) with $a = 65.83$ and $b = 0.17$ (Fig. 9a); hybrid rates vs. incubation $[O_2]$ produced fits with $a = 76.26$ and $b = 0.067$ (Fig. 9b).

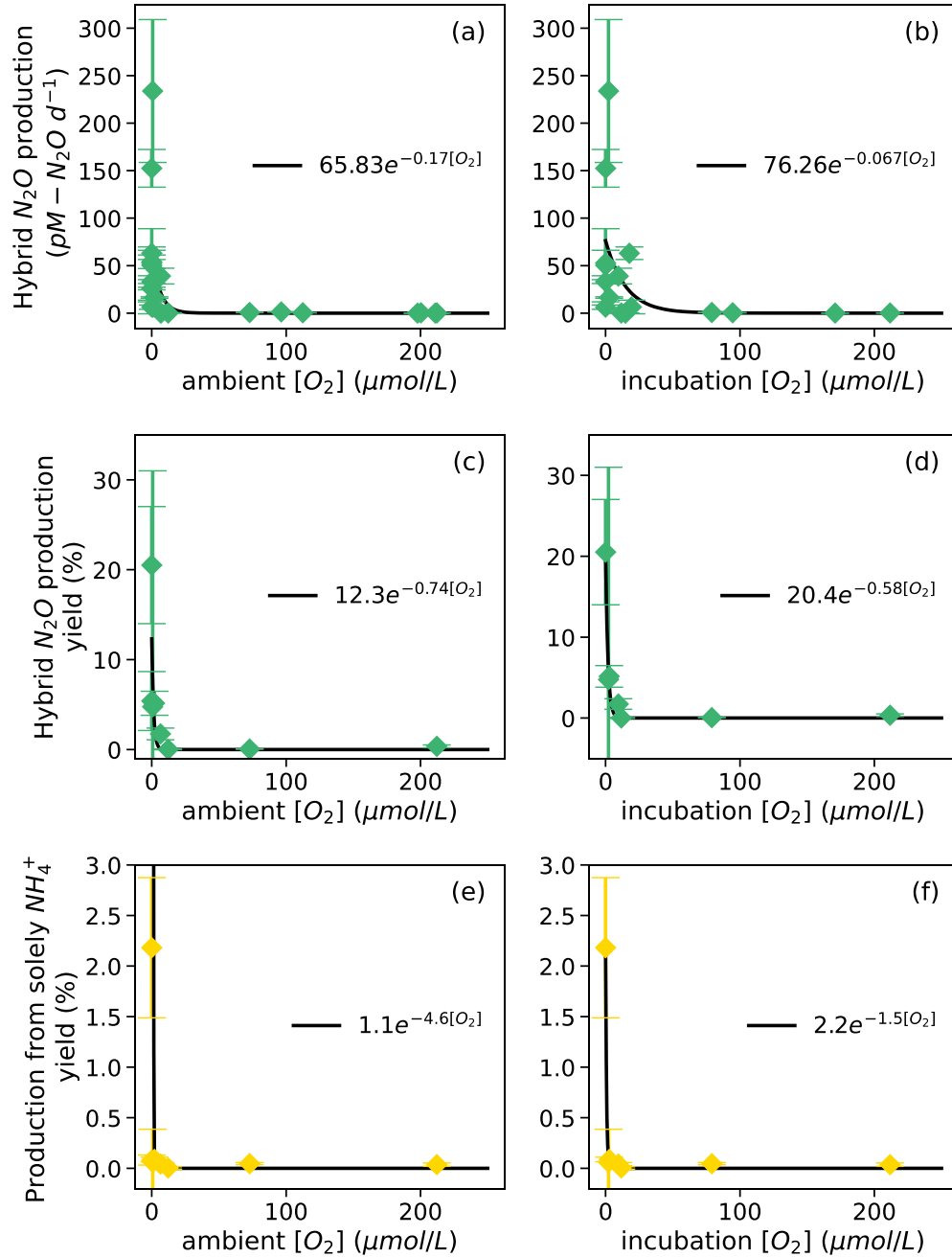


Figure 9. Hybrid N_2O production rates (a,b), N_2O yield (%) during hybrid production (c, d), and N_2O yield (%) during production from solely NH_4^+ (e, f) along a range of ambient $[O_2]$ measured by a Seabird sensor for the Niskin bottles from which samples were taken (a, c, e) and $[O_2]$ measured by chemiluminescent optodes mounted inside incubation bottles (b, d, f). Error bars are calculated from 100 model optimizations, varying key parameters by up to 25%. Yields are only calculated at stations and depths where rates of NH_3 oxidation are greater than 0. Curves of form $\mathbf{rate} = \mathbf{ae}^{-b[O_2]}$ are fit through the data (black lines); values of a and b are shown in white boxes in each plot.

The rate of N_2O production from solely NH_4^+ also decreased exponentially with increasing dissolved $[O_2]$. The highest rates of N_2O production from solely NH_4^+ occurred in the secondary chlorophyll maximum at station PS3 (Table S4), where dissolved oxygen was below detection.

N_2O yield during production from solely NH_4^+ also exhibited exponentially decreasing relationships with dissolved $[O_2]$ (Fig. 9e–f). To ensure mass balance in terms of NH_4^+ consumption (Fig. S9), N_2O yield (%) during production from solely NH_4^+ was calculated as:

$$\text{yield (\%)} = \frac{2 \left[N_2O \text{ from solely } NH_4^+ \left(nM N_2O / \text{day} \right) \right]}{2 \left[N_2O \text{ from solely } NH_4^+ \left(nM N_2O / \text{day} \right) \right] + \text{hybrid } N_2O \left(nM N_2O / \text{day} \right) + NH_3 \text{ oxidation } \left(nM N / \text{day} \right)} \quad (22)$$

where N_2O production from solely NH_4^+ is in units of $nM N_2O/\text{day}$, hybrid N_2O production is in units of $nM N_2O/\text{day}$, and NH_3 oxidation to NO_2^- is in units of $nM N/\text{day}$. This assumes that the formation of N_2O from solely NH_4^+ draws two nitrogen atoms from the NH_4^+ pool, while hybrid N_2O production and the oxidation of NH_4^+ to NO_2^- each draw one atom from the NH_4^+ pool (Fig. S9). Following the same convention, N_2O yield (%) during hybrid production was calculated as:

$$\text{yield (\%)} = \frac{\text{hybrid } N_2O \left(nM N_2O / \text{day} \right)}{2 \left[N_2O \text{ from solely } NH_4^+ \left(nM N_2O / \text{day} \right) \right] + \text{hybrid } N_2O \left(nM N_2O / \text{day} \right) + NH_3 \text{ oxidation } \left(nM N / \text{day} \right)} \quad (23)$$

The maximum N_2O yield from hybrid production was $21 \pm 7\%$ (Fig. 9c, d). while the maximum N_2O yield during production from solely NH_4^+ was $2.2 \pm 0.7\%$ (Fig. 9e, f). N_2O yield during production from solely NH_4^+ declined more sharply with increased O_2 than N_2O yield during hybrid production (Fig. 9c–f).

Figure 4 d: the trace for ammonium oxidation differs from the corresponding trace in Figure 3 a. **Thank you for catching this. Figure 3a is correct. Not sure what happened with Figure 4d (now Figure 6d) but we corrected it (see response to comment on Figure 4 above).**

Discussion:

Because the study is very complex, it would be beneficial for the discussion to begin with a paragraph that summarizes the dominant findings, rather than jumping into the deep end form the get go. In this regard, I would also get N_2O production from denitrification out of the way first because it was the dominant flux, then discuss hybrid production. I find it interesting as well that production from hydroxylamine was virtually absent except at the surface – I think this merits more emphasis.

Thank you for this suggestion. We added a summary paragraph at the beginning of the discussion, and we changed the order of the discussion to 1) N_2O production from denitrification, 2) hybrid production, 3) production from solely NH_4^+ .

4 Discussion

In this study, we found that N_2O production from denitrification was the dominant source of N_2O both within the ODZ and in the upper oxycline. Hybrid N_2O production was a smaller but significant contributor to N_2O in the upper oxycline, and the primary source of N_2O in the deep oxycline. N_2O production from solely NH_4^+ – which includes N_2O from hydroxylamine oxidation, hybrid production with cellular NO_2^- , and nitrifier–denitrification with cellular NO_2^- – was negligible everywhere except surface waters. Our findings of equal formation of $^{45}N_2O^\alpha$ and $^{45}N_2O^\beta$ in most experiments indicate that N^α retains an equal proportion of NO_2^- and NH_4^+ –derived N during hybrid production, which may imply that hybrid N_2O production exhibits a constant $\delta(^{15}N^{sp})$. All of the processes measured in this study exhibited a strong dependence on

dissolved oxygen, although denitrification was less inhibited by dissolved oxygen than previous work would suggest.

Section 4.3: I get that MOST N₂O is produced by denitrification and 1/5 from hybrid production. Is that what is also inferred from natural abundance measurements, in these proportions? Curious minds want to know

Yes, this is indeed what we inferred from natural abundance measurements. Based on natural abundance site preference, we found that the near-surface [N₂O] maximum in was likely to be comprised of ~20% N₂O produced via nitrification or archaeal N₂O production and ~80% N₂O produced via denitrification (Kelly et al., 2021). We added this to the beginning of section 4.1 (formerly section 4.3).

Based on our rate data, N₂O production from NO₃⁻ is the dominant source of N₂O in both the near-surface [N₂O] maximum and the anoxic ODZ core. This agrees well with natural abundance isotopocule measurements in the ETNP, which indicate that the near surface [N₂O] maximum is likely to be comprised of ~80% N₂O produced via denitrification and ~20% N₂O produced via nitrification or archaeal N₂O production, producing a local minimum in $\delta(^{15}\text{N}^{\text{sp}})$ (Kelly et al., 2021).

Line 642: What do you mean by “allowed?” Need better wording.

Here we’re alluding to natural abundance measurements indicating that N₂O production from NO₃⁻ could be an important source of N₂O in the anoxic core of ODZs, as long as it has a positive $\delta(^{15}\text{N}^{\text{sp}})$. As you know, denitrification is usually assigned $\delta(^{15}\text{N}^{\text{sp}}) \approx 0\text{‰}$ (Sutka et al., 2006), but some strains of denitrifying bacteria can produce N₂O with $\delta(^{15}\text{N}^{\text{sp}}) > 0\text{‰}$ (Toyoda et al., 2005; Wang et al., 2023). And so can denitrifying fungi (Sutka et al., 2008; Rohe et al., 2014; Yang et al., 2014; Lazo-Murphy et al., 2022). So, given that there are several potential sources of N₂O production from NO₃⁻ with a positive $\delta(^{15}\text{N}^{\text{sp}})$, the importance of N₂O production from NO₃⁻ in this study agrees with natural abundance work.

Natural abundance isotopomer work has shown that N₂O production from NO₃⁻ could be an important source of N₂O in the anoxic core of ODZs, as long as it has a positive $\delta(^{15}\text{N}^{\text{sp}})$ (Casciotti et al., 2018; Kelly et al., 2021; Monreal et al., 2022). While denitrification is generally accepted to produce N₂O with $\delta(^{15}\text{N}^{\text{sp}}) \approx 0\text{‰}$ (Sutka et al., 2006; other refs), some strains of denitrifying bacteria can produce N₂O with $\delta(^{15}\text{N}^{\text{sp}}) = 10\text{--}22\text{‰}$ (Toyoda et al., 2005; Wang et al., 2023) and denitrifying fungi produce N₂O with $\delta(^{15}\text{N}^{\text{sp}}) = 35\text{--}37\text{‰}$ (Sutka et al., 2008; Rohe et al., 2014; Yang et al., 2014; Lazo-Murphy et al., 2022). Here, the dominance of N₂O production from ¹⁵N–NO₃⁻, combined with parallel natural abundance isotopomer studies, suggest that strains of denitrifying bacteria and fungi that produce N₂O with a high site preference may be important contributors to N₂O in the core of ODZs.

Line 650: qualify “this” , you mean the notion that internal pool are processed, not external...?

Yes, exactly. We changed “this” to “N₂O production from NO₃⁻ that utilizes an internal NO₂⁻ pool”.

N₂O production from NO₃⁻ that utilizes an internal NO₂⁻ pool is currently left out of most biogeochemical models of nitrogen cycling in and around oxygen-deficient zones (Bianchi et al., 2023), and modeling work is needed that includes this as a source of N₂O.

Line 600: Reader is left hanging: What are the implications for mechanisms of production? Need a concluding sentence for the paragraph to bridge it to the next, or simply amalgamate with the following paragraph.

We re-wrote this paragraph and the following text to reflect the fact that most of our experiments actually have *equal* formation of $^{45}\text{N}_2\text{O}^\alpha$ and $^{45}\text{N}_2\text{O}^\beta$, and thus $f=0.5$, which would imply that hybrid $\delta(^{15}\text{N}^{\text{sp}})$ would *not* vary in most of the tested conditions.

Although our data do not allow us to comment directly on the enzymatic machinery of hybrid N_2O formation, our data can be used to theorize hypothetical pathways for hybrid N_2O production. Firstly, we see much higher rates of hybrid production using ambient NO_2^- (Pathway 3 in Wan et al., 2023) than hybrid production using cellular NO_2^- (Pathway 2 in Wan et al., 2023). Again, this agrees with the results of Wan et al. (2023), who see higher rates of hybrid formation from extracellular NO_2^- within the range of $[^{15}\text{N}-\text{NH}_4^+]/[\text{NO}_2^-]$ covered by our experiments. In our model, hybrid N_2O production is operationally defined as a 1:1 combination of N derived from NH_4^+ and NO_2^- , which is generally consistent with previous work (Stieglmeier et al., 2014). Any combination of N derived from NO_2^- with a second N derived from NO_2^- would be included in the modeled quantity of N_2O production from NO_2^- ; likewise, any combination of N derived from NH_4^+ with a second N derived from NH_4^+ would be included in the N_2O production from solely NH_4^+ . The question, then, is what reaction would be specific enough to have one N derived from each substrate, but not specific enough to govern ^{15}N placement in the resulting N_2O ? One such reaction could be the combination of NH_4^+ and NO_2^- to form a symmetrical intermediate such as hyponitrite (HONNOH or $^-\text{ONNO}^-$ in its deprotonated form), which reacts to form N_2O via breakage of one of the N–O bonds, resulting in N_2O that contains a 1:1 ratio of $\text{NH}_4^+:\text{NO}_2^-$. With a precursor such as hyponitrite, equal formation of $^{45}\text{N}_2\text{O}^\alpha$ and $^{45}\text{N}_2\text{O}^\beta$ could be achieved with non-selective N–O bond breakage.

These findings of equal $^{45}\text{N}_2\text{O}$ production have important implications for the natural abundance $\delta(^{15}\text{N}^{\text{sp}})$ of N_2O produced by the hybrid N_2O process. Assuming that hybrid N_2O production proceeds through a symmetrical intermediate in which NH_4^+ and NO_2^- are paired in a 1:1 ratio, we can model $\delta(^{15}\text{N}^{\text{sp}})$ as:

$$\begin{aligned} \delta(^{15}\text{N}^{\text{sp}}) &= \delta(^{15}\text{N}^\alpha) - \delta(^{15}\text{N}^\beta) \\ &= [f\delta(^{15}\text{N} - \text{NO}_2^-) + (1 - f)\delta(^{15}\text{N} - \text{NH}_4^+)] - [(1 - f)\delta(^{15}\text{N} - \text{NO}_2^-) + f\delta(^{15}\text{N} - \text{NH}_4^+) - \varepsilon] \end{aligned} \quad (24)$$

where f is the proportion of the α nitrogen derived from NO_2^- and the proportion of the β nitrogen derived from NH_4^+ , and ε is the fractionation factor associated with $\text{N}^\beta\text{--O}$ bond breakage. If $f \neq 1/2$, hybrid $\delta(^{15}\text{N}^{\text{sp}})$ retains a dependence on the $\delta(^{15}\text{N})$ of the substrates – or more accurately, the difference in $\delta(^{15}\text{N})$ of the two substrates; if the $\delta(^{15}\text{N})$ of the substrates is equal, it will cancel out regardless of f . If $\delta(^{15}\text{N}-\text{NH}_4^+) > \delta(^{15}\text{N}-\text{NO}_2^-)$, as is generally the case in the secondary nitrite maximum (Buchwald et al., 2015; Casciotti, 2016), then low values of f should produce high hybrid $\delta(^{15}\text{N}^{\text{sp}})$, and high values of f should produce low hybrid $\delta(^{15}\text{N}^{\text{sp}})$ (Fig. 10). If, however, $f = 1/2$, as was the case for most experimental depths in this study, hybrid $\delta(^{15}\text{N}^{\text{sp}})$ should depend only on ε and not the isotopic composition of each substrate. This means that a

$\delta(^{15}\text{N}^{\text{sp}})$ endmember could potentially be established for hybrid N_2O production, even though hybrid N_2O production draws from different substrate pools. More studies are needed to determine the $\delta(^{15}\text{N}^{\text{sp}})$ of N_2O produced by ammonia-oxidizing archaea under a range of conditions.

Paragraph at line 605: Reads like something that should be in results section.

We moved this text down to our paragraph where we address the unequal production of $^{45}\text{N}_2\text{O}^\alpha$ and $^{45}\text{N}_2\text{O}^\beta$ at certain depths, which anchored significant relationships between f and ambient $[\text{O}_2]$ and potential density anomaly (σ_θ). The oxygen and potential density gradients may be proxies for changing archaeal community compositions at different depths in the water column, which may exhibit different patterns of incorporation of NO_2^- -derived N and NH_4^+ -derived N into N^α and N^β . It is also possible that we sampled a different “hybrid” N_2O -producing process at these depths, such as fungal co-denitrification (Shoun et al., 2012), which may proceed via a different pathway from archaeal hybrid N_2O production.

The unequal production of $^{45}\text{N}_2\text{O}^\alpha$ and $^{45}\text{N}_2\text{O}^\beta$ observed at certain depths led to values of f significantly different from 0.5 (Table S4). At these depths, N^α retained a different proportion of nitrogen derived from NO_2^- and NH_4^+ than N^β , causing $^{45}\text{N}_2\text{O}^\alpha$ and $^{45}\text{N}_2\text{O}^\beta$ to diverge. The depths with $f \neq 0.5$ anchored significant relationships between f and ambient $[\text{O}_2]$ ($R^2 = 0.84$, $p < 0.001$; Fig. S10a) and potential density anomaly (σ_θ) ($R^2 = 0.72$, $p < 0.001$; Fig. S10b). The oxygen and potential density gradients may be proxies for changing archaeal community compositions at different depths in the water column, which may exhibit different patterns of incorporation of NO_2^- -derived N and NH_4^+ -derived N into N^α and N^β . It is also possible that we sampled a different “hybrid” N_2O -producing process at these depths, such as fungal co-denitrification (Shoun et al., 2012), which may proceed via a different pathway from archaeal hybrid N_2O production.

Line 610: Articulate fully for readers to catch up again “findings of unequal alpha vs. beta production during hybrid pathway have implications for interpretation of the natural abundance isotopes of N_2O produced by hybrid process.”

We now write:

The equal formation of $^{45}\text{N}_2\text{O}^\alpha$ and $^{45}\text{N}_2\text{O}^\beta$ led to values of f within error of 0.5 in most of our experiments (Table S4), and the mean value of f across all stations and depths was 0.5 ± 0.2 . This means that during hybrid N_2O production, half of the N^α atoms were derived from NO_2^- , and half were derived from NH_4^+ (likewise for N^β).

Paragraph at line 670: I don't understand why the results here should be different than cited study.

(Ji et al., 2018) did not include hybrid N_2O production in their estimates of N_2O yield. We added this to the text.

The maximum N_2O yield for hybrid production (21%; Fig. 8c,d) was an order of magnitude higher than previous estimates of N_2O yields during NH_3 oxidation from ETSP and ETNP, which did not include hybrid N_2O production (Ji et al., 2018).

I remain perplexed by the following: In Figure S8, there is NO production of $^{45}\text{N}_2\text{O}$ from addition of $^{15}\text{NH}_4^+$ at 100 m at station 1, yet there is reportedly 50 nM/day N_2O production from

the hybrid pathway at this depth... Am I fundamentally misunderstanding something about the experimental design? The hybrid pathway requires some input from $^{15}\text{NH}_4^+$ which should be detected as $^{45}\text{N}_2\text{O}$?

We can understand why this would be confusing. The model solves for the same rates of hybrid N_2O production in the $^{15}\text{NH}_4^+$ and $^{15}\text{NO}_2^-$ experiments. In this case, there is high $^{45}\text{N}_2\text{O}$ production in the $^{15}\text{NO}_2^-$ experiment but very little $^{45}\text{N}_2\text{O}$ production in the $^{15}\text{NH}_4^+$, so the model finds an intermediate value. Given that the $^{15}\text{N-NO}_2^-$ spike was added at a higher concentration (5 μM) than the $^{15}\text{N-NH}_4^+$ spike (0.5 μM), it is feasible that the $^{15}\text{N-NO}_2^-$ generated a greater $^{45}\text{N}_2\text{O}$ signal than the $^{15}\text{N-NH}_4^+$ experiment.

References

- Babbin, A. R., Bianchi, D., Jayakumar, A., and Ward, B. B.: Rapid nitrous oxide cycling in the suboxic ocean, *Science*, 348, 1127–1129, <https://doi.org/10.1126/science.aaa8380>, 2015.
- Bianchi, D., Weber, T. S., Kiko, R., and Deutsch, C.: Global niche of marine anaerobic metabolisms expanded by particle microenvironments, *Nat. Geosci.*, 11, 263–268, <https://doi.org/10.1038/s41561-018-0081-0>, 2018.
- Bianchi, D., McCoy, D., and Yang, S.: Formulation, optimization, and sensitivity of NitrOMZv1.0, a biogeochemical model of the nitrogen cycle in oceanic oxygen minimum zones, *Geosci. Model Dev.*, 16, 3581–3609, <https://doi.org/10.5194/gmd-16-3581-2023>, 2023.
- Bourbonnais, A., Letscher, R. T., Bange, H. W., Échevin, V., Larkum, J., Mohn, J., Yoshida, N., and Altabet, M. A.: N_2O production and consumption from stable isotopic and concentration data in the Peruvian coastal upwelling system, *Glob. Biogeochem. Cycles*, 31, 678–698, <https://doi.org/10.1002/2016GB005567>, 2017.
- Bourbonnais, A., Chang, B. X., Sonnerup, R. E., Doney, S. C., and Altabet, M. A.: Marine N_2O cycling from high spatial resolution concentration, stable isotopic and isotopomer measurements along a meridional transect in the eastern Pacific Ocean, *Front. Mar. Sci.*, 10, 2023.
- Breitburg, D., Levin, L. A., Oschlies, A., Grégoire, M., Chavez, F. P., Conley, D. J., Garçon, V., Gilbert, D., Gutiérrez, D., Isensee, K., Jacinto, G. S., Limburg, K. E., Montes, I., Naqvi, S. W. A., Pitcher, G. C., Rabalais, N. N., Roman, M. R., Rose, K. A., Seibel, B. A., Telszewski, M., Yasuhara, M., and Zhang, J.: Declining oxygen in the global ocean and coastal waters, *Science*, 359, eaam7240, <https://doi.org/10.1126/science.aam7240>, 2018.
- Brennkmeijer, C. A. M. and Röckmann, T.: Mass spectrometry of the intramolecular nitrogen isotope distribution of environmental nitrous oxide using fragment-ion analysis, *Rapid Commun. Mass Spectrom.*, 13, 2028–2033, [https://doi.org/10.1002/\(SICI\)1097-0231\(19991030\)13:20<2028::AID-RCM751>3.0.CO;2-J](https://doi.org/10.1002/(SICI)1097-0231(19991030)13:20<2028::AID-RCM751>3.0.CO;2-J), 1999.
- Buchwald, C., Santoro, A. E., Stanley, R. H. R., and Casciotti, K. L.: Nitrogen cycling in the secondary nitrite maximum of the eastern tropical North Pacific off Costa Rica, *Glob. Biogeochem. Cycles*, 29, 2061–2081, <https://doi.org/10.1002/2015GB005187>, 2015.

Busecke, J. J. M., Resplandy, L., Ditkovsky, S. J., and John, J. G.: Diverging Fates of the Pacific Ocean Oxygen Minimum Zone and Its Core in a Warming World, *AGU Adv.*, 3, e2021AV000470, <https://doi.org/10.1029/2021AV000470>, 2022.

Cabré, A., Marinov, I., Bernardello, R., and Bianchi, D.: Oxygen minimum zones in the tropical Pacific across CMIP5 models: mean state differences and climate change trends, *Biogeosciences*, 12, 5429–5454, <https://doi.org/10.5194/bg-12-5429-2015>, 2015.

Carini, P., Dupont, C. L., and Santoro, A. E.: Patterns of thaumarchaeal gene expression in culture and diverse marine environments, *Environ. Microbiol.*, 20, 2112–2124, <https://doi.org/10.1111/1462-2920.14107>, 2018.

Casciotti, K. L.: Nitrite isotopes as tracers of marine N cycle processes, *Philos. Transact. A Math. Phys. Eng. Sci.*, 374, 20150295, <https://doi.org/10.1098/rsta.2015.0295>, 2016.

Casciotti, K. L., Forbes, M., Vedamati, J., Peters, B. D., Martin, T. S., and Mordy, C. W.: Nitrous oxide cycling in the Eastern Tropical South Pacific as inferred from isotopic and isotopomeric data, *Deep Sea Res. Part II Top. Stud. Oceanogr.*, 156, 155–167, <https://doi.org/10.1016/j.dsr2.2018.07.014>, 2018.

Codispoti, L. A. and Christensen, J. P.: Nitrification, denitrification and nitrous oxide cycling in the eastern tropical South Pacific ocean, *Mar. Chem.*, 16, 277–300, [https://doi.org/10.1016/0304-4203\(85\)90051-9](https://doi.org/10.1016/0304-4203(85)90051-9), 1985.

Cohen, Y. and Gordon, L. I.: Nitrous oxide production in the Ocean, *J. Geophys. Res. Oceans*, 84, 347–353, <https://doi.org/10.1029/JC084iC01p00347>, 1979.

Dalsgaard, T., Stewart, F. J., Thamdrup, B., Brabandere, L. D., Revsbech, N. P., Ulloa, O., Canfield, D. E., and DeLong, E. F.: Oxygen at Nanomolar Levels Reversibly Suppresses Process Rates and Gene Expression in Anammox and Denitrification in the Oxygen Minimum Zone off Northern Chile, *mBio*, 5, e01966-14, <https://doi.org/10.1128/mBio.01966-14>, 2014.

Farías, L., Castro-González, M., Cornejo, M., Charpentier, J., Faúndez, J., Boontanon, N., and Yoshida, N.: Denitrification and nitrous oxide cycling within the upper oxycline of the eastern tropical South Pacific oxygen minimum zone, *Limnol. Oceanogr.*, 54, 132–144, <https://doi.org/10.4319/lo.2009.54.1.0132>, 2009.

Farías, L., Faúndez, J., Fernández, C., Cornejo, M., Sanhueza, S., and Carrasco, C.: Biological N₂O fixation in the Eastern South Pacific Ocean and marine cyanobacterial cultures, *PloS One*, 8, e63956, <https://doi.org/10.1371/journal.pone.0063956>, 2013.

Frame, C. H. and Casciotti, K. L.: Biogeochemical controls and isotopic signatures of nitrous oxide production by a marine ammonia-oxidizing bacterium, *Biogeosciences*, 7, 2695–2709, <https://doi.org/10.5194/bg-7-2695-2010>, 2010.

Frame, C. H., Lau, E., Nolan, E. J. I., Goepfert, T. J., and Lehmann, M. F.: Acidification Enhances Hybrid N₂O Production Associated with Aquatic Ammonia-Oxidizing Microorganisms, *Front. Microbiol.*, 7, <https://doi.org/10.3389/fmicb.2016.02104>, 2017.

Frey, C., Bange, H. W., Achterberg, E. P., Jayakumar, A., Löscher, C. R., Arévalo-Martínez, D. L., León-Palmero, E., Sun, M., Sun, X., Xie, R. C., Oleynik, S., and Ward, B. B.: Regulation of nitrous oxide production in low-oxygen waters off the coast of Peru, *Biogeosciences*, 17, 2263–2287, <https://doi.org/doi.org/10.5194/bg-17-2263-2020>, 2020.

Frey, C., Sun, X., Szemlerski, L., Casciotti, K. L., Garcia-Robledo, E., Jayakumar, A., Kelly, C. L., Lehmann, M. F., and Ward, B. B.: Kinetics of nitrous oxide production from ammonia oxidation in the Eastern Tropical North Pacific, *Limnol. Oceanogr.*, 68, 424–438, <https://doi.org/10.1002/lno.12283>, 2023.

Garcia, H. E. and Gordon, L. I.: Oxygen Solubility in Seawater: Better Fitting Equations, *Limnol. Oceanogr.*, 37, 1307–1312, 1992.

Goreau, T. J., Kaplan, W. A., Wofsy, S. C., McElroy, M. B., Valois, F. W., and Watson, S. W.: Production of NO₂- and N₂O by Nitrifying Bacteria at Reduced Concentrations of Oxygen, *Appl. Environ. Microbiol.*, 40, 526–532, <https://doi.org/10.1128/aem.40.3.526-532.1980>, 1980.

Granger, J. and Sigman, D. M.: Removal of nitrite with sulfamic acid for nitrate N and O isotope analysis with the denitrifier method, *Rapid Commun. Mass Spectrom.*, 23, 3753–3762, <https://doi.org/10.1002/rcm.4307>, 2009.

Ji, Q., Babbin, A. R., Jayakumar, A., Oleynik, S., and Ward, B. B.: Nitrous oxide production by nitrification and denitrification in the Eastern Tropical South Pacific oxygen minimum zone, *Geophys. Res. Lett.*, 42, 10,755–10,764, <https://doi.org/10.1002/2015GL066853>, 2015.

Ji, Q., Buitenhuis, E., Suntharalingam, P., Sarmiento, J. L., and Ward, B. B.: Global Nitrous Oxide Production Determined by Oxygen Sensitivity of Nitrification and Denitrification, *Glob. Biogeochem. Cycles*, 32, 1790–1802, <https://doi.org/10.1029/2018GB005887>, 2018.

Kaiser, J., Park, S., Boering, K. A., Brenninkmeijer, C. A. M., Hilker, A., and Röckmann, T.: Mass spectrometric method for the absolute calibration of the intramolecular nitrogen isotope distribution in nitrous oxide, *Anal. Bioanal. Chem.*, 378, 256–269, <https://doi.org/10.1007/s00216-003-2233-2>, 2004.

Kantnerová, K., Hattori, S., Toyoda, S., Yoshida, N., Emmenegger, L., Bernasconi, S. M., and Mohn, J.: Clumped isotope signatures of nitrous oxide formed by bacterial denitrification, *Geochim. Cosmochim. Acta*, 328, 120–129, <https://doi.org/10.1016/j.gca.2022.05.006>, 2022.

Kelly, C. L., Travis, N. M., Baya, P. A., and Casciotti, K. L.: Quantifying Nitrous Oxide Cycling Regimes in the Eastern Tropical North Pacific Ocean With Isotopomer Analysis, *Glob. Biogeochem. Cycles*, 35, e2020GB006637, <https://doi.org/10.1029/2020GB006637>, 2021.

Kim, K.-R. and Craig, H.: Two-isotope characterization of N₂O in the Pacific Ocean and constraints on its origin in deep water, *Nature*, 347, 58–61, <https://doi.org/10.1038/347058a0>, 1990.

- Kozłowski, J. A., Kits, K. D., and Stein, L. Y.: Comparison of Nitrogen Oxide Metabolism among Diverse Ammonia-Oxidizing Bacteria, *Front. Microbiol.*, 7, <https://doi.org/10.3389/fmicb.2016.01090>, 2016.
- Kraft, B., Jehmlich, N., Larsen, M., Bristow, L. A., Könneke, M., Thamdrup, B., and Canfield, D. E.: Oxygen and nitrogen production by an ammonia-oxidizing archaeon, *Science*, <https://doi.org/10.1126/science.abe6733>, 2022.
- Lancaster, K. M., Caranto, J. D., Majer, S. H., and Smith, M. A.: Alternative Bioenergy: Updates to and Challenges in Nitrification Metalloenzymology, *Joule*, 2, 421–441, <https://doi.org/10.1016/j.joule.2018.01.018>, 2018.
- Lazo-Murphy, B. M., Larson, S., Staines, S., Bruck, H., McHenry, J., Bourbonnais, A., and Peng, X.: Nitrous oxide production and isotopomer composition by fungi isolated from salt marsh sediments, *Front. Mar. Sci.*, 9, 2022.
- Lipschultz, F.: Chapter 31 - Isotope Tracer Methods for Studies of the Marine Nitrogen Cycle, in: *Nitrogen in the Marine Environment (Second Edition)*, edited by: Capone, D. G., Bronk, D. A., Mulholland, M. R., and Carpenter, E. J., Academic Press, San Diego, 1345–1384, <https://doi.org/10.1016/B978-0-12-372522-6.00031-1>, 2008.
- Magyar, P. M., Orphan, V. J., and Eiler, J. M.: Measurement of rare isotopologues of nitrous oxide by high-resolution multi-collector mass spectrometry, *Rapid Commun. Mass Spectrom.*, 30, 1923–1940, <https://doi.org/10.1002/rcm.7671>, 2016.
- Martens-Habbena, W., Qin, W., Horak, R. E. A., Urakawa, H., Schauer, A. J., Moffett, J. W., Armbrust, E. V., Ingalls, A. E., Devol, A. H., and Stahl, D. A.: The production of nitric oxide by marine ammonia-oxidizing archaea and inhibition of archaeal ammonia oxidation by a nitric oxide scavenger, *Environ. Microbiol.*, 17, 2261–2274, <https://doi.org/10.1111/1462-2920.12677>, 2015.
- McIlvin, M. R. and Altabet, M. A.: Chemical Conversion of Nitrate and Nitrite to Nitrous Oxide for Nitrogen and Oxygen Isotopic Analysis in Freshwater and Seawater, *Anal. Chem.*, 77, 5589–5595, <https://doi.org/10.1021/ac050528s>, 2005.
- Monreal, P. J., Kelly, C. L., Travis, N. M., and Casciotti, K. L.: Identifying the Sources and Drivers of Nitrous Oxide Accumulation in the Eddy-Influenced Eastern Tropical North Pacific Oxygen-Deficient Zone, *Glob. Biogeochem. Cycles*, 36, e2022GB007310, <https://doi.org/10.1029/2022GB007310>, 2022.
- Naqvi, S. W. A., Jayakumar, D. A., Narvekar, P. V., Naik, H., Sarma, V. V. S. S., D'Souza, W., Joseph, S., and George, M. D.: Increased marine production of N₂O due to intensifying anoxia on the Indian continental shelf, *Nature*, 408, 346–349, <https://doi.org/10.1038/35042551>, 2000.
- Nelder, J. A. and Mead, R.: A Simplex Method for Function Minimization, *Comput. J.*, 7, 308–313, <https://doi.org/10.1093/comjnl/7.4.308>, 1965.

- Oschlies, A., Brandt, P., Stramma, L., and Schmidtko, S.: Drivers and mechanisms of ocean deoxygenation, *Nat. Geosci.*, 11, 467–473, <https://doi.org/10.1038/s41561-018-0152-2>, 2018.
- Popp, B. N., Westley, M. B., Toyoda, S., Miwa, T., Dore, J. E., Yoshida, N., Rust, T. M., Sansone, F. J., Russ, M. E., Ostrom, N. E., and Ostrom, P. H.: Nitrogen and oxygen isotopomeric constraints on the origins and sea-to-air flux of N₂O in the oligotrophic subtropical North Pacific gyre, *Glob. Biogeochem. Cycles*, 16, 12-1-12–10, <https://doi.org/10.1029/2001GB001806>, 2002.
- Rahn, T. and Wahlen, M.: A reassessment of the global isotopic budget of atmospheric nitrous oxide, *Glob. Biogeochem. Cycles*, 14, 537–543, <https://doi.org/10.1029/1999GB900070>, 2000.
- Rohe, L., Anderson, T.-H., Braker, G., Flessa, H., Giesemann, A., Lewicka-Szczebak, D., Wrage-Mönnig, N., and Well, R.: Dual isotope and isotopomer signatures of nitrous oxide from fungal denitrification – a pure culture study, *Rapid Commun. Mass Spectrom.*, 28, 1893–1903, <https://doi.org/10.1002/rcm.6975>, 2014.
- Shoun, H., Fushinobu, S., Jiang, L., Kim, S.-W., and Wakagi, T.: Fungal denitrification and nitric oxide reductase cytochrome P450_{nor}, *Philos. Trans. Biol. Sci.*, 367, 1186–1194, 2012.
- Si, Y., Zhu, Y., Sanders, I., Kinkel, D. B., Purdy, K. J., and Trimmer, M.: Direct biological fixation provides a freshwater sink for N₂O, *Nat. Commun.*, 14, 6775, <https://doi.org/10.1038/s41467-023-42481-2>, 2023.
- Sigman, D. M., Casciotti, K. L., Andreani, M., Barford, C., Galanter, M., and Böhlke, J. K.: A Bacterial Method for the Nitrogen Isotopic Analysis of Nitrate in Seawater and Freshwater, *Anal. Chem.*, 73, 4145–4153, <https://doi.org/10.1021/ac010088e>, 2001.
- Smith, C., Nicholls, Z. R. J., Armour, K., Collins, W., Dufresne, J.-L., Frame, D., Lunt, D. J., Mauritsen, M. D., Palmer, M. D., Watanabe, M., Wild, M., and Zhang, H.: The Earth’s Energy Budget, Climate Feedbacks, and Climate Sensitivity Supplementary Material, in: *Climate Change 2021: The Physical Science Basis. Contribution of Working Group I to the Sixth Assessment Report of the Intergovernmental Panel on Climate Change*, edited by: Masson-Delmotte, V., Zhai, P., Pirani, A., Connors, S. L., Péan, C., Berger, S., Caud, N., Chen, Y., Goldfarb, L., Gomis, M. I., Huang, M., Leitzell, K., Lonnoy, E., Matthews, J. B. R., Maycock, T. K., Waterfield, T., Yelekçi, O., Yu, R., and Zhou, B., Cambridge University Press, Cambridge, United Kingdom, 2021.
- Smriga, S., Ciccarese, D., and Babbín, A. R.: Denitrifying bacteria respond to and shape microscale gradients within particulate matrices, *Commun. Biol.*, 4, 570, <https://doi.org/10.1038/s42003-021-02102-4>, 2021.
- Stein, L. Y.: Insights into the physiology of ammonia-oxidizing microorganisms, *Curr. Opin. Chem. Biol.*, 49, 9–15, <https://doi.org/10.1016/j.cbpa.2018.09.003>, 2019.
- Stein, L. Y. and Yung, Y. L.: Production, Isotopic Composition, and Atmospheric Fate of Biologically Produced Nitrous Oxide, *Annu. Rev. Earth Planet. Sci.*, 31, 329–356, <https://doi.org/10.1146/annurev.earth.31.110502.080901>, 2003.

Stieglmeier, M., Mooshammer, M., Kitzler, B., Wanek, W., Zechmeister-Boltenstern, S., Richter, A., and Schleper, C.: Aerobic nitrous oxide production through N-nitrosating hybrid formation in ammonia-oxidizing archaea, *ISME J.*, 8, 1135–1146, <https://doi.org/10.1038/ismej.2013.220>, 2014.

Stramma, L., Johnson, G. C., Sprintall, J., and Mohrholz, V.: Expanding Oxygen-Minimum Zones in the Tropical Oceans, *Science*, 320, 655–658, <https://doi.org/10.1126/science.1153847>, 2008.

Sun, X., Jayakumar, A., Tracey, J. C., Wallace, E., Kelly, C. L., Casciotti, K. L., and Ward, B. B.: Microbial N₂O consumption in and above marine N₂O production hotspots, *ISME J.*, 15, 1434–1444, <https://doi.org/10.1038/s41396-020-00861-2>, 2021.

Sutka, R. L., Ostrom, N. E., Ostrom, P. H., Gandhi, H., and Breznak, J. A.: Nitrogen isotopomer site preference of N₂O produced by *Nitrosomonas europaea* and *Methylococcus capsulatus* Bath, *Rapid Commun. Mass Spectrom. RCM*, 17, 738–745, <https://doi.org/10.1002/rcm.968>, 2003.

Sutka, R. L., Ostrom, N. E., Ostrom, P. H., Gandhi, H., and Breznak, J. A.: Nitrogen isotopomer site preference of N₂O produced by *Nitrosomonas europaea* and *Methylococcus capsulatus* Bath, *Rapid Commun. Mass Spectrom.*, 18, 1411–1412, <https://doi.org/10.1002/rcm.1482>, 2004.

Sutka, R. L., Ostrom, N. E., Ostrom, P. H., Breznak, J. A., Gandhi, H., Pitt, A. J., and Li, F.: Distinguishing Nitrous Oxide Production from Nitrification and Denitrification on the Basis of Isotopomer Abundances, *Appl. Environ. Microbiol.*, 72, 638–644, <https://doi.org/10.1128/AEM.72.1.638-644.2006>, 2006.

Sutka, R. L., Adams, G. C., Ostrom, N. E., and Ostrom, P. H.: Isotopologue fractionation during N₂O production by fungal denitrification, *Rapid Commun. Mass Spectrom.*, 22, 3989–3996, <https://doi.org/10.1002/rcm.3820>, 2008.

Tian, H., Xu, R., Canadell, J. G., Thompson, R. L., Winiwarter, W., Suntharalingam, P., Davidson, E. A., Ciais, P., Jackson, R. B., Janssens-Maenhout, G., Prather, M. J., Regnier, P., Pan, N., Pan, S., Peters, G. P., Shi, H., Tubiello, F. N., Zaehle, S., Zhou, F., Arneeth, A., Battaglia, G., Berthet, S., Bopp, L., Bouwman, A. F., Buitenhuis, E. T., Chang, J., Chipperfield, M. P., Dangal, S. R. S., Dlugokencky, E., Elkins, J. W., Eyre, B. D., Fu, B., Hall, B., Ito, A., Joos, F., Krummel, P. B., Landolfi, A., Laruelle, G. G., Lauerwald, R., Li, W., Lienert, S., Maavara, T., MacLeod, M., Millet, D. B., Olin, S., Patra, P. K., Prinn, R. G., Raymond, P. A., Ruiz, D. J., van der Werf, G. R., Vuichard, N., Wang, J., Weiss, R. F., Wells, K. C., Wilson, C., Yang, J., and Yao, Y.: A comprehensive quantification of global nitrous oxide sources and sinks, *Nature*, 586, 248–256, <https://doi.org/10.1038/s41586-020-2780-0>, 2020.

Toyoda, S. and Yoshida, N.: Determination of nitrogen isotopomers of nitrous oxide on a modified isotope ratio mass spectrometer, *Anal. Chem.*, 71, 4711–4718, <https://doi.org/10.1021/ac9904563>, 1999.

Toyoda, S., Yoshida, N., Miwa, T., Matsui, Y., Yamagishi, H., Tsunogai, U., Nojiri, Y., and Tsurushima, N.: Production mechanism and global budget of N₂O inferred from its isotopomers

in the western North Pacific, *Geophys. Res. Lett.*, 29, 7-1-7-4, <https://doi.org/10.1029/2001GL014311>, 2002.

Toyoda, S., Mutobe, H., Yamagishi, H., Yoshida, N., and Tanji, Y.: Fractionation of N₂O isotopomers during production by denitrifier, *Soil Biol. Biochem.*, 37, 1535–1545, <https://doi.org/10.1016/j.soilbio.2005.01.009>, 2005.

Toyoda, S., Yoshida, O., Yamagishi, H., Fujii, A., Yoshida, N., and Watanabe, S.: Identifying the origin of nitrous oxide dissolved in deep ocean by concentration and isotopocule analyses, *Sci. Rep.*, 9, 1–9, <https://doi.org/10.1038/s41598-019-44224-0>, 2019.

Toyoda, S., Kakimoto, T., Kudo, K., Yoshida, N., Sasano, D., Kosugi, N., Ishii, M., Kameyama, S., Inagawa, M., Yoshikawa-Inoue, H., Nishino, S., Murata, A., Ishidoya, S., and Morimoto, S.: Distribution and Production Mechanisms of N₂O in the Western Arctic Ocean, *Glob. Biogeochem. Cycles*, 35, e2020GB006881, <https://doi.org/10.1029/2020GB006881>, 2021.

Toyoda, S., Terajima, K., Yoshida, N., Yoshikawa, C., Makabe, A., Hashihama, F., and Ogawa, H.: Extensive Accumulation of Nitrous Oxide in the Oxygen Minimum Zone in the Bay of Bengal, *Glob. Biogeochem. Cycles*, 37, e2022GB007689, <https://doi.org/10.1029/2022GB007689>, 2023.

Trimmer, M., Chronopoulou, P.-M., Maanoja, S. T., Upstill-Goddard, R. C., Kitidis, V., and Purdy, K. J.: Nitrous oxide as a function of oxygen and archaeal gene abundance in the North Pacific, *Nat. Commun.*, 7, 13451–13451, <https://doi.org/10.1038/ncomms13451>, 2016.

Vajrala, N., Martens-Habben, W., Sayavedra-Soto, L. A., Schauer, A., Bottomley, P. J., Stahl, D. A., and Arp, D. J.: Hydroxylamine as an intermediate in ammonia oxidation by globally abundant marine archaea, *Proc. Natl. Acad. Sci. U. S. A.*, 110, 1006–1011, 2013.

Virtanen, P., Gommers, R., Oliphant, T. E., Haberland, M., Reddy, T., Cournapeau, D., Burovski, E., Peterson, P., Weckesser, W., Bright, J., van der Walt, S. J., Brett, M., Wilson, J., Millman, K. J., Mayorov, N., Nelson, A. R. J., Jones, E., Kern, R., Larson, E., Carey, C. J., Polat, İ., Feng, Y., Moore, E. W., VanderPlas, J., Laxalde, D., Perktold, J., Cimrman, R., Henriksen, I., Quintero, E. A., Harris, C. R., Archibald, A. M., Ribeiro, A. H., Pedregosa, F., and van Mulbregt, P.: SciPy 1.0: fundamental algorithms for scientific computing in Python, *Nat. Methods*, 17, 261–272, <https://doi.org/10.1038/s41592-019-0686-2>, 2020.

Wan, X. S., Sheng, H.-X., Liu, L., Shen, H., Tang, W., Zou, W., Xu, M. N., Zheng, Z., Tan, E., Chen, M., Zhang, Y., Ward, B. B., and Kao, S.-J.: Particle-associated denitrification is the primary source of N₂O in oxic coastal waters, *Nat. Commun.*, 14, 8280, <https://doi.org/10.1038/s41467-023-43997-3>, 2023a.

Wan, X. S., Hou, L., Kao, S.-J., Zhang, Y., Sheng, H.-X., Shen, H., Tong, S., Qin, W., and Ward, B. B.: Pathways of N₂O production by marine ammonia-oxidizing archaea determined from dual-isotope labeling, *Proc. Natl. Acad. Sci.*, 120, e2220697120, <https://doi.org/10.1073/pnas.2220697120>, 2023b.

- Wang, R. Z., Lonergan, Z. R., Wilbert, S. A., Eiler, J. M., and Newman, D. K.: Widespread detoxifying NO reductases impart a distinct isotopic fingerprint on N₂O under anoxia, *Microbiology*, <https://doi.org/10.1101/2023.10.13.562248>, 2023.
- Westley, M. B., Yamagishi, H., Popp, B. N., and Yoshida, N.: Nitrous oxide cycling in the Black Sea inferred from stable isotope and isotopomer distributions, *Deep Sea Res. Part II Top. Stud. Oceanogr.*, 53, 1802–1816, <https://doi.org/10.1016/j.dsr2.2006.03.012>, 2006.
- Wrage, N., Velthof, G. L., Van Beusichem, M. L., and Oenema, O.: Role of nitrifier denitrification in the production of nitrous oxide, *Soil Biol. Biochem.*, 33, 1723–1732, [https://doi.org/10.1016/S0038-0717\(01\)00096-7](https://doi.org/10.1016/S0038-0717(01)00096-7), 2001.
- Yamagishi, H., Westley, M. B., Popp, B. N., Toyoda, S., Yoshida, N., Watanabe, S., Koba, K., and Yamanaka, Y.: Role of nitrification and denitrification on the nitrous oxide cycle in the eastern tropical North Pacific and Gulf of California, *J. Geophys. Res. Biogeosciences*, 112, <https://doi.org/10.1029/2006JG000227>, 2007.
- Yang, H., Gandhi, H., Ostrom, N. E., and Hegg, E. L.: Isotopic Fractionation by a Fungal P450 Nitric Oxide Reductase during the Production of N₂O, *Environ. Sci. Technol.*, 48, 10707–10715, <https://doi.org/10.1021/es501912d>, 2014.
- Zumft, W. G.: Cell biology and molecular basis of denitrification, *Microbiol. Mol. Biol. Rev.*, <https://doi.org/10.1128/membr.61.4.533-616.1997>, 1997.